

This document is confidential and is proprietary to the American Chemical Society and its authors. Do not copy or disclose without written permission. If you have received this item in error, notify the sender and delete all copies.

Mono-alkyl phosphinic acids as ligands in nanocrystal synthesis

Journal:	<i>ACS Nano</i>
Manuscript ID	nn-2021-08966m.R3
Manuscript Type:	Article
Date Submitted by the Author:	n/a
Complete List of Authors:	Dhaene, Evert; Ghent University, Chemistry Pokratath, Rohan; University of Basel Aalling-Frederiksen, Olivia ; University of Copenhagen, Department of Chemistry Jensen, Kirsten; University of Copenhagen, Department of Chemistry Smet, Philippe; Universiteit Gent, LumiLab, Department of Solid State Sciences De Buysser, Klaartje; Universiteit Gent, Inorganic and physical Chemistry De Roo, Jonathan; Universität Basel, Departement Chemie

SCHOLARONE™
Manuscripts

Mono-alkyl Phosphinic Acids as Ligands in Nanocrystal Synthesis

Evert Dhaene,¹ Rohan Pokratath,² Olivia Aalling-Frederiksen,³ Kirsten M. Ø. Jensen,³ Philippe

F. Smet,⁴ Klaartje De Buysser,¹ Jonathan De Roo^{2*}

¹ Department of Chemistry, Ghent University, Gent B-9000, Belgium

² Department of Chemistry, University of Basel, Basel CH-4058, Switzerland

³ Department of Chemistry, University of Copenhagen, 2100 Copenhagen Ø, Denmark

⁴ Department of Solid State Sciences, Ghent University, Gent B-9000, Belgium

* Corresponding author: Jonathan De Roo, Jonathan.DeRoo@unibas.ch

Abstract

Ligands play a crucial role in the synthesis of colloidal nanocrystals. Nevertheless, only a handful molecules are currently used, oleic acid being the most typical example. Here, we show that mono-alkyl phosphinic acids are another interesting ligand class, forming metal complexes with a reactivity that is intermediate between the traditional carboxylates and phosphonates. We first present the synthesis of *n*-hexyl, 2-ethylhexyl, *n*-tetradecyl, *n*-octadecyl, and oleyl phosphinic acid. These compounds are suitable ligands for high-temperature nanocrystal synthesis (240-300°C) since, in contrast to phosphonic acids, they do not form anhydride oligomers. Consequently, CdSe quantum dots synthesized with octadecylphosphinic acid are conveniently purified, and their UV-Vis spectrum is free from background scattering. The CdSe nanocrystals have a low polydispersity and a photoluminescence quantum yield up to 18%. Furthermore, we could synthesize CdSe and CdS nanorods using phosphinic acid ligands, with high shape purity. We conclude that the reactivity towards TOP-S and TOP-Se precursors decreases in the series: cadmium carboxylate > cadmium phosphinate > cadmium phosphonate. By introducing a third and intermediate class of surfactants, we enhance the versatility of surfactant-assisted syntheses.

Keywords

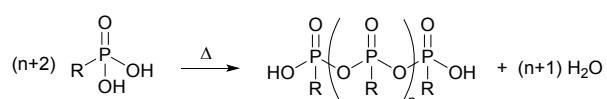
nanocrystals, quantum dots, nanorods, ligands, phosphinic acids, surface chemistry

Introduction

Colloidal nanocrystals (NCs) are composed of nanosized (< 100 nm) inorganic crystalline cores, capped with (in)organic ligands on the surface.¹⁻² The most common organic ligands used in nanocrystal synthesis are also surfactants, with long alkyl chains and a polar binding group. For very small nanocrystals (< 10 nm) the classical concepts of colloidal stability do not apply and such nanocrystals have an equilibrium solubility. This *colloidal solubility* is determined by the binding group and the alkyl chain of the surfactant, the nanocrystal core size and the solvent.³⁻⁸ Apart from providing solubility to the final nanocrystals, surfactants also play an important role in nanocrystal synthesis, regulating the nucleation and growth rates.⁹⁻¹¹ Finally, controlling the surface chemistry has proven key to many (if not all) nanocrystal applications.^{2,}

Despite the crucial role of ligands, it is striking that most colloidal synthesis methods use the same types of surfactants: oleic acid, oleylamine and octadecylphosphonic acid being the most common. While thiols are great ligands for metals,¹² and metal chalcogenides,¹³ they are not thermally stable. Indeed, they are often used as sulphur precursors.¹⁴ Metal oleates are stable metal precursors for quantum dot syntheses at relatively low temperatures (240 °C).¹⁵⁻¹⁶ At higher temperatures they often decompose to metals or metal oxides.¹⁷⁻¹⁸ Oleylamine is a typical L-type ligand and binds usually in a dynamic fashion.¹⁹ In very specific systems, oleylamine can be a tightly bound ligand.²⁰⁻²¹ Phosphonates and phosphates are among the strongest ligands available and easily displace carboxylic acids,^{13, 22-23} especially when designed as multidentate ligands on a scaffold.²⁴⁻²⁵ Phosphonic acids are also the ligands of choice for high temperature (> 300 °C) quantum dot syntheses. Peng *et al.* used a mixture of saturated phosphonic acids to synthesize CdE (E = S, Se or Te) NCs and nanorods.²⁶ Later, wurtzite CdSe quantum dots were made by Owen *et al* using only *n*-octadecylphosphonic acid.²⁷ Carbone *et al.* used this strategy to obtain CdSe/CdS dot-in-rod structures.²⁸ Motivated by these reports, we recently developed

1
2
3 the synthesis of a library of phosphonic acid ligands,²³ including the highly soluble
4 oleylphosphonic acid. Zhang *et al.* then used oleylphosphonic acid to synthesize CsPbBr₃
5 nanocrystals.²⁹⁻³⁰ Although phosphonic acids thus allow to make a variety of nanocrystal
6 (hetero)structures, they are not without a drawback. We find that phosphonic acids are unstable
7 at high temperature (300 °C), dehydrating to phosphonic acid anhydrides within 30 min (Figure
8 S1). In nanocrystal syntheses with phosphonic acid ligands, phosphonic acid anhydrides are
9 indeed often formed as by-products, and even retrieved on the nanocrystal surface.²⁹⁻³⁵ The
10 formal dehydration is shown in Scheme 1. Many nanocrystal syntheses contain dehydration
11 agents (e.g., phosphine chalcogenide or acyl bromide), thus forming other co-products than
12 water. Since phosphonic acids have two OH moieties, this reaction can proceed further, forming
13 oligomers.³² Over time, a macroscopic gel is often observed in nanocrystal samples with the
14 phosphonic acid anhydride oligomer present.³¹ These may be a reason why reproducing certain
15 nanocrystal reactions can prove challenging.



33
34
35
36
37
38 **Scheme 1.** Formal dehydration of phosphonic acids. In practice, often a dehydration agent is also present in the
39 reaction mixture.
40

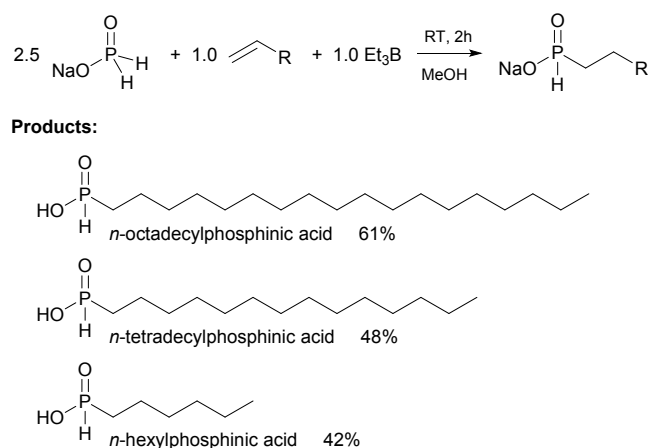
41
42 Another origin of irreproducibility is the use of impure reagents. In 2008, Wang *et al.*
43 discovered the role of di-*n*-octylphosphonic acid and *n*-octylphosphonic acid on the formation
44 of CdSe nanorods and nanowires.³⁶⁻³⁸ These molecules were present as impurities in
45 commercially available tri-*n*-octylphosphine oxide (TOPO). Phosphonic acids were thus clearly
46 an alternative ligand class, but only the di-substituted variants received further attention.³⁹ For
47 example, bis(2,2,4-trimethylpentyl)phosphonic acid phosphonic acid was explored as co-ligand
48 by Mulvaney *et al.*⁴⁰⁻⁴² Recently, Kovalenko *et al.* synthesized CsPbX₃ from PbBr₂,
49 didodecyldimethylammonium halide and cesium di-isooctylphosphinate.⁴³ The di-alkyl
50
51
52
53
54
55
56
57
58
59
60

1
2
3 phosphinate did not end up as a ligand on the nanocrystal surface, presumably due to its high
4 steric hindrance.⁴⁴⁻⁴⁵ Mono-substituted alkylphosphinic acids have not yet been explored in
5
6 nanocrystal synthesis.
7
8

9
10 Here, we put forward mono-alkyl phosphinic acids as an alternative ligand class, similar to
11 carboxylic acids and phosphonic acids. After presenting the ligand synthesis for several selected
12 substrates, we proceed to show the intermediate reactivity of the phosphinic acids in CdSe
13 quantum dot syntheses. The nanocrystals synthesized with phosphinic acids are also easier to
14 purify since there is no gel formation. Very small (2-3 nm) CdSe quantum dots with low
15 polydispersity and high photoluminescence quantum yields can be easily accessed with
16 phosphinic acids ligands. CdSe and CdS nanorods were also synthesized using phosphinic
17 acids, whereby the rods showed high purity and uniformity. We have thus presented a ligand
18 class that is truly a worthy alternative to carboxylic acids and phosphonic acids, as X-type
19 ligands in nanocrystal synthesis.
20
21
22
23
24
25
26
27
28
29
30
31
32
33
34
35
36
37

38 **Results and Discussion**

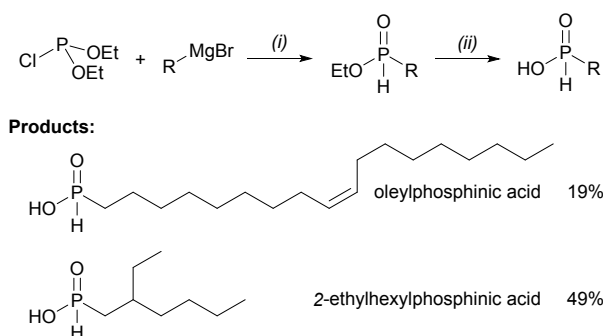
39
40
41
42 **Phosphinic acid synthesis.** To synthesize mono-alkyl phosphinic acids, suitable as ligands for
43 nanocrystal synthesis, we identified two main methods.⁴⁶ Method I involves the addition of an
44 alkene to hypophosphorous acid (H_3PO_2) or sodium hypophosphite (NaH_2PO_2). Double
45 alkylation can occur and is typically avoided by an excess of phosphorus reagent. Several
46 variations exist with different radical initiators, solvents and reagents concentrations.^{36, 46-49} We
47 found the general protocol of Montchamp *et al.* (Scheme 2) most convenient to synthesize our
48 target compounds; *n*-hexyl-, *n*-tetradecyl-, and *n*-octadecylphosphinic acid. The method can be
49 easily performed on multigram scale and uses inexpensive reagents. We recrystallized the
50 products to a high purity (>99%, based on ^{31}P NMR).
51
52
53
54
55
56
57
58
59
60



18 **Scheme 2.** Method I to synthesize mono n -alkyl phosphinic acids and the obtained products with the yield
19 indicated.

20
21
22
23 We also targeted more complex phosphinic acids such as oleylphosphinic acid and 2-
24 ethylhexylphosphinic acid. The oleyl fragment is ubiquitous in nanocrystals synthesis due to its
25 high solubility and the high colloidal solubility it provides to nanocrystals. A branched chain
26 provides also very high colloidal solubility as shown by Peng *et al.*³ To synthesize
27 oleylphosphinic acid we first prepared the corresponding terminal alkene, since it is not
28 commercially available. We preferred to start by reducing oleic acid to oleyl alcohol to avoid
29 the *trans* isomer present in technical oleyl alcohol. The reduction is performed with Li[AlH₄]
30 according to Grela *et al.*⁵⁰ The alcohol was subsequently transformed in either a mesylate or a
31 bromide to function as a good leaving group during the E₁ elimination towards the terminal
32 alkene.⁵¹⁻⁵² Upon addition of KO^tBu, oleyl mesylate remained stable but oleyl bromide fully
33 converted to the terminal alkene. Unfortunately, method I yielded a mixture of the desired linear
34 oleylphosphinic acid and the undesired, branched octadec-1-en-9-ylphosphinic acid. For this
35 reason, we used method II, where oleylbromide is converted into a Grignard reagent, and the
36 latter reacts with diethyl chlorophosphite (Scheme 3).^{46, 53} Both the oleyl and the branched
37 compound cannot be recrystallized and are purified (>95% according ³¹P NMR) by column
38 chromatography as the ethyl ester, before being hydrolysed to the target product.

39
40
41
42
43
44
45
46
47
48
49
50
51
52
53
54
55
56
57
58
59
60



15 **Scheme 3.** Method II to synthesize more complex phosphinic acids and the obtained products. Conditions: (i)
16 overnight at 50 °C in dry THF, then 2 h at room temperature in conc. HCl and water. (ii) 1.15 eq of TMS-Br,
17 overnight in dry DCM, then dry MeOH, 6h, 40 °C.

18
19
20 **CdSe quantum dot synthesis.** Wurtzite CdSe quantum dots are typically synthesized at 300
21 °C from cadmium *n*-alkylphosphonate, which is formed *in situ* from cadmium oxide and *n*-
22 alkylphosphonic acid. Oligomeric phosphonic acid anhydride is a co-product of this reaction,
23 and it was observed previously that the final quantum dot suspension turns in a macroscopic
24 gel over time.³¹ Drijvers *et al.* managed to significantly reduce the formation of the oligomeric
25 phosphonic acid anhydride upon addition of oleyl alcohol to the reaction.³¹ The alcohol forms
26 an ester with one of the two hydroxyl groups of the phosphonic acid, thus inhibiting oligomer
27 formation. Since also gel formation was thus inhibited, it was suggested that the gel formation
28 is related to the presence of phosphonic acid anhydride oligomer, although the exact mechanism
29 of gelation is unknown. We hypothesize that we avoid the problem entirely by using mono-
30 alkyl phosphinic acids.
31
32
33
34
35
36
37
38
39
40
41
42
43
44
45

46 Similar to the phosphonic acid based strategy,²⁶⁻²⁷ we first dissolved CdO with two equivalents
47 of octadecylphosphinic acid in TOPO. Phosphinic acid requires higher temperatures to dissolve
48 the CdO, compared to phosphonic acid. This is most likely due to the lower acidity of
49 alkylphosphinic acid (pK_a in $H_2O \approx 3.1$) compared to alkylphosphonic acid (pK_a in $H_2O \approx 2.4$
50 and 7.7).⁵⁴ After dissolution of CdO, TOP-Se is injected at 300 °C and CdSe quantum dots are
51 rapidly formed (Figure 1). After 10 minutes the reaction mixture is cooled down and the
52 nanocrystals are easily purified by precipitation/redispersion cycles with acetone/toluene as
53
54
55
56
57
58
59
60

1
2
3 antisolvent/solvent. We did not observe any oils or gels. Although the nanocrystals have already
4 ripened (see next section), the size dispersion is still quite low; 8 % (size according to TEM:
5 3.46 ± 0.28 nm ($\mu \pm \sigma$)), see Figure 1B and Figure S2. Given the small nanocrystal size, we
6 turned to x-ray Pair Distribution Function analysis (PDF) to determine the crystal structure.⁵⁵
7
8 The refinement using the wurtzite crystal structure gave a much better fit ($R_w = 0.17$) than the
9 refinement with the zincblende crystal structure ($R_w = 0.50$), see Figure 1C and Figure S3. From
10 the wurtzite refinement, we determined the crystallite size to be 2.9 nm (Figure S3). The
11 nanocrystal dispersion is also free from organic impurities as attested by NMR. In the ^1H NMR
12 spectrum we observe the broadened signature of a bound alkyl chain (Figure 1D).⁵⁶ In Diffusion
13 Ordered Spectroscopy (DOSY), we find only a single diffusing species (apart from toluene),
14 see Figure 1E. The diffusion coefficient is 93.78 ± 0.16 $\mu\text{m}^2 \text{s}^{-1}$, corresponding to a
15 solvodynamic diameter of 7.8 nm (which agrees quite well with the nanocrystal core size +
16 twice the length of the octadecyl chain (approx. 2 nm). There is no evidence of an oligomeric
17 impurity while we find this impurity in the DOSY spectrum of CdSe quantum dots synthesized
18 with octadecylphosphonic acid (Figure S4).
19
20
21
22
23
24
25
26
27
28
29
30
31
32
33
34
35
36
37
38
39
40
41
42
43
44
45
46
47
48
49
50
51
52
53
54
55
56
57
58
59
60

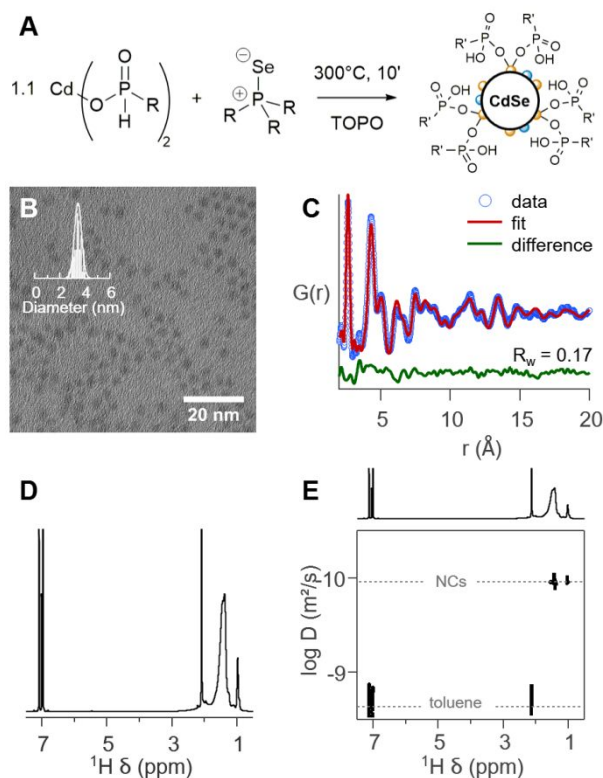


Figure 1. CdSe quantum dots synthesized with *n*-octadecylphosphonic acid. (A) general reaction scheme, (B) TEM image with histogram, (C) x-ray PDF analysis showing a single phase refinement with the wurtzite crystal structure. (D) ^1H NMR spectrum, and (E) DOSY NMR spectrum.

In the ^{31}P NMR spectrum, we observe a broadened resonance around 25 ppm, assigned to bound ligands (Figure S5A). In the ^1H NMR spectrum, the ratio of the methylene ($-\text{CH}_2-$) and methyl (CH_3-) integral (3:30) is lower than expected for an octadecyl chain (3:34), see Figure S5A. This suggests that a shorter chain is present. After stripping the native ligands with trifluoroacetic acid, we do not observe the expected P-H resonance of *n*-alkylphosphonic acid in the ^1H NMR spectrum (Figure S5B). Also in ^{31}P NMR spectrum, the resonance of the stripped ligand does not agree with the reference spectrum of alkylphosphonic acid. It does match with the reference spectrum of alkylphosphonic acid. These result suggests that during the synthesis a portion of the octadecylphosphonic acids oxidized and that the solvent (TOPO) decomposed and formed octylphosphonic acid. There is literature precedent for the latter.³⁴⁻³⁵ Alternatively, we stripped the native ligands with chlorotrimethylsilane, and we observe 2

1
2
3 major resonances matching with trimethylsilyl hydrogen phosphonate and bis(trimethylsilyl)
4 phosphonate (Figure S5C).²⁹ Quenching the stripping products with anhydrous methanol results
5
6 in a single resonance matching with alkylphosphonic acid (Figure S5C). In addition, MS
7
8 analysis of these products is consistent with the presence of two compounds:
9
10 octadecylphosphonic acid (major component) and octylphosphonic acid (minor component),
11
12 see Figure S6.
13
14
15
16
17

18 **Kinetic comparison with phosphonic and carboxylic acid ligands.** According to UV-Vis
19 spectroscopy, CdSe quantum dots synthesized with phosphonic acid (5.4 nm) are larger than
20 the ones synthesized with phosphinic acids (3.3 nm), see Figure S7. This could be related to the
21 precursor conversion kinetics of the reactions since it is established that faster reactions yield
22 more, but smaller, particles.^{15, 57} To investigate this in more detail, we followed the reaction
23 kinetics and also compared with carboxylic acid ligands (Figure 2). We took several reaction
24 aliquots, quantified and diluted them for quantitative UV-Vis spectroscopy analysis. In case of
25 the mono-alkyl phosphinic acids, the kinetic traces showed a good batch-to-batch
26 reproducibility, see Figure S8. The nanocrystal size was calculated from the position of the first
27 excitonic peak, and the absorption at 340 nm was used to determine the yield.⁵⁸ From the yield
28 and the size, we calculate the number of particles. We performed this analysis at 300 °C for
29 both phosphinic and phosphonic acid ligands, and at 240 °C for both phosphinic and carboxylic
30 acid ligands. These temperatures were chosen since 300 °C is the common reaction temperature
31 for phosphonic acid ligands, and 240 °C is usual for carboxylic acids.
32
33
34
35
36
37
38
39
40
41
42
43
44
45
46
47
48
49

50
51 For phosphonic acids, the yield shows comparable kinetics to the previous reports for the used
52 Cd:Se stoichiometry (Figure 2).³³ After an induction time (where no particles are observed), the
53 number of particles increases over the course of the reaction suggesting continuous nucleation
54 instead of burst nucleation. Continuous nucleation was recently found to be a quite general
55 feature of nanocrystal synthesis, applicable to Ir, Pd, InP and CdSe nanocrystals.^{10, 59-61} The
56
57
58
59
60

1
2
3 particles grow steadily from 3.4 to 5.4 nm, while the valley-to-peak ratio slightly increases.
4
5 Given the difficulty in calculating an exact polydispersity from UV-Vis spectroscopy, we
6
7 choose to present the valley-to-peak ratio, as a measure for the polydispersity at a given size.⁶²
8
9
10 A low valley-to-peak ratio is characteristic for a monodisperse sample, but for a constant
11
12 polydispersity, the valley-to-peak ratio increases with nanocrystal size. As such, we do not
13
14 interpret the slight increase in valley-to-peak ratio over the course of the reaction as ripening.
15
16
17
18
19
20
21
22
23
24
25
26
27
28
29
30
31
32
33
34
35
36
37
38
39
40
41
42
43
44
45
46
47
48
49
50
51
52
53
54
55
56
57
58
59
60

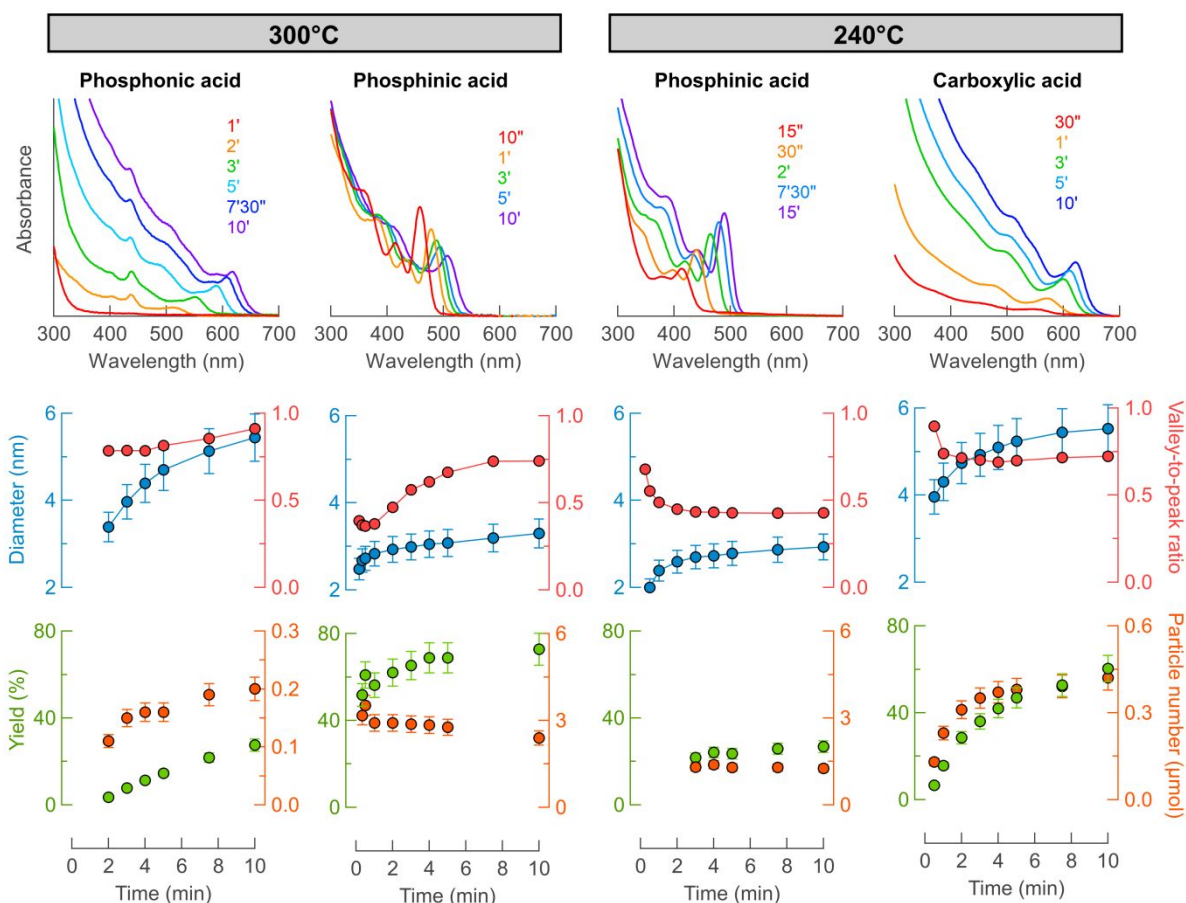


Figure 2. UV-Vis absorption spectra of CdSe quantum dots synthesized from a CdX₂ salt and TOP-Se, at two temperatures, with X being either phosphonate, phosphinate, or carboxylate. Besides the used ligand and temperature, all other reaction parameters remained identical. Also the extracted mean diameter, the valley-to-peak ratio, the reaction yield and the number of particles are plotted for the four different reactions. Note that the scale changes for the number of particles across the four figures.

With phosphinic acids we did not observe an induction time. At 300 °C, particles are formed almost instantaneously and the first particles are also much smaller (2.5 nm) than the first particles observed for phosphonic acids (3.4 nm). The reaction reaches also a higher yield after 10 min (72 % vs 28 % for phosphinic and phosphonic acids respectively). Most of the reaction with phosphinic acids is already completed after 2 min. However, the particles continue to grow, presumably through a ripening mechanism since the number of particles slightly

1
2
3 decreases and the valley-to-ratio significantly increases (Figure 2). Clearly, phosphinic acids
4 allow for a higher reactivity than phosphonic acids (faster yield development). Furthermore,
5 the formed particles with phosphinic acids are particularly small (< 3 nm, a size range that is
6 usually difficult to access⁶³) and the particles have sharp first excitonic features (FWHM at 2.7
7 eV: 260 meV).⁶⁴⁻⁶⁵ An additional advantage of the phosphinic acids for kinetic analysis is the
8 long term stability of the dispersions. While kinetic analysis has to be performed immediately
9 for the phosphonic acids samples due to partial gelation (causing scattering in UV-Vis
10 spectroscopy), the phosphinic acid samples give identical results after 20 weeks, see Figure S9.

11
12
13
14
15
16
17
18
19
20
21
22 At 240 °C (Figure 2), the yield development seems more sluggish for phosphinic acids
23 compared to carboxylic acids, suggesting that cadmium phosphinates are less reactive than
24 cadmium carboxylates. Note that we could not determine the yield (and thus the particle
25 number) for the aliquots taken until 2 min since the absorption at 340 nm is not size independent
26 for these very small sizes (< 2.7 nm). For carboxylic acids, we see again continuous nucleation
27 (increasing particle number as the yield increases, see Figure 2), while we do not observe such
28 a feature for the phosphinic acids. The particle number remains constant while the yield
29 increases slightly. We do not observe ripening for the phosphinic acids at 240°C. Instead, the
30 size dispersion focuses (indicated by a decreasing valley-to-peak ratio) while the particles are
31 growing. Again, very small particles (2-3 nm) are obtained with sharp excitonic features
32 (FWHM at 2.54 eV: 244 meV). We conclude that the phosphinic acid ligands lead to particle
33 ensembles with narrow size dispersions and that their reactivity is intermediate between
34 phosphonic and carboxylic acids.
35
36
37
38
39
40
41
42
43
44
45
46
47
48
49
50
51

52
53 **Photoluminescence properties.** For crude CdSe (i.e., unpurified reaction mixture) synthesized
54 with oleic acid at 240 °C, we obtained a photoluminescence quantum yield (PLQY) of 5.6%
55 (Figure S10A). After purification, this decreased to 0.5%, an effect which has been observed
56 before in the literature.^{64, 66-68} For the CdSe particles synthesized with phosphonic acids, we
57
58
59
60

1
2
3 obtained a very low PLQY of 0.2% for the crude and < 0.1% after purification (Figure S10B).
4
5 Concerning CdSe synthesized with phosphinic acid under identical conditions at 300 °C, we
6
7 obtained a PLQY of 18% for the crude aliquot at 10 seconds (first excitonic peak at 2.7 eV),
8
9 with a FWHM of 150 meV (Figure S10C). After ripening (10 min), the PLQY is 16.1 ± 0.8 %
10
11 (average and error determined from four independent syntheses) and after purification we
12
13 measure only 3%. For CdSe synthesized with phosphinic acid at 240 °C, there is more
14
15 variability and we measure a PLQY of 6-11% for the crude after 15 min reaction (first excitonic
16
17 peak at 2.53 eV) and the FWHM was 130 meV (Figure S10D). After purification, the PLQY
18
19 reduced to 4%. A full photophysical analysis is outside the scope of this work, but it is clear
20
21 that under identical conditions, CdSe nanocrystal synthesized with phosphinic acids have a
22
23 higher PLQY than the ones synthesized with phosphonic acids. Their values are up to par with
24
25 the state of the art of unshelled CdSe nanocrystals (typically less than 15%, with the exception
26
27 of Bawendi *et al.*⁶⁹ and Jasieniak *et al.*⁷⁰), and with quite narrow line-widths.^{66, 68-77}
28
29
30
31
32
33

34 **Synthesis of CdSe and CdS nanorods.** Phosphonic acids are also used in reactions to obtain
35
36 anisotropic nanocrystals, such as nanorods. Buhro *et al.* synthesized CdSe nanorods by reacting
37
38 cadmium tetradecylphosphonate with TOP-Se in the presence of di-*n*-octylphosphinic acid
39
40 (DOPA).³⁶ The TOP-Se is injected at 275 °C but the temperature is allowed to drop to 250 °C
41
42 during the growth of the rods. The amount of added DOPA controls the aspect ratio. We
43
44 successfully reproduced this method but we obtained, apart from the intended rods, also
45
46 tetrapods (Figure 3 and Figure S11). When we perform the same reaction with cadmium
47
48 tetradecylphosphinate, no rods but regular quantum dots are obtained (Figure S12). The reaction
49
50 reaches maximum yield at 1 min, after which the particles start ripening. We attribute this result
51
52 to the higher reactivity of cadmium phosphinate, depleting all the precursor already during the
53
54 formation of the seeds. Therefore, we lowered also the injection temperature to 250 °C, and
55
56 particles with a slightly anisotropic shape are obtained (Figure S13). Decreasing the
57
58
59
60

temperature even further (TOP-Se is injected at 250 °C and the temperature is allowed to drop to 225 °C for the growth), results in nanorods albeit with a small aspect ratio and some tetrapods are again observed, see Figure 3 and Figure S14.

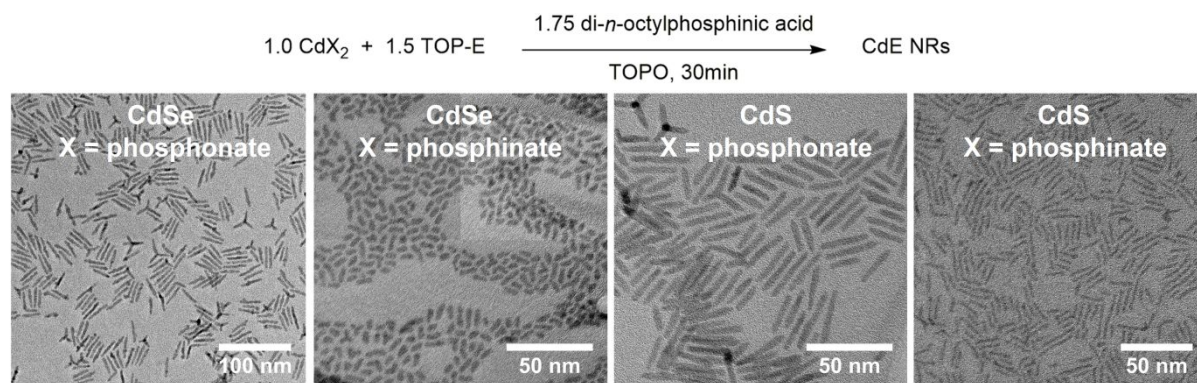


Figure 3. CdS and CdSe nanorods synthesized with phosphonic and phosphinic acid.

TOP-S has a higher phosphor-chalcogen bond dissociation energy (BDE) than TOP-Se.¹⁸ We thus hypothesized that cadmium phosphinate would be more suitable to grow CdS rods since the higher BDE of TOP-S would decrease the precursor conversion rate. Gratifyingly, CdS rods were indeed obtained when TOP-S was injected at 275 °C and the rods were grown at 250 °C (Figure 3). The nanorods were highly monodisperse (width: 2.4 ± 0.3 nm, and length: 14.6 ± 2.8 nm) and the sample had >99% shape purity (Figure S15). In comparison, the control experiment with phosphonic acid failed several times. In one case the reaction resulted in CdS rods but they were contaminated with tetrapods (Figure 3). Furthermore, the rods with phosphinic acid were easier to purify due to the absence of a gel.

Discussion. We have introduced another surfactant class: mono-alkylphosphinic acids. Several features make this ligand class stand out. (1) Both the kinetics experiments and the nanorod synthesis have confirmed that cadmium phosphinates have intermediate reactivity, reacting slower with TOP-E precursors than cadmium carboxylates but faster than cadmium phosphonates. This provides the nanochemist with an additional handle on the reaction kinetics.

1
2
3 Before, tuning the precursor conversion kinetics was limited to the chalcogen or pnictogen
4 precursor,^{16, 59, 78-80} but now we gain an additional handle on the kinetics through the metal
5 precursor salt. (2) Reactions with phosphinic acids are not plagued by the occurrence of oligo-
6 anhydride. The latter can manifest itself by inducing macroscopic gel formation, or as
7 background scattering in UV-Vis spectroscopy or SAXS (small-angle x-ray scattering).
8 Therefore, we expect that this class of mono-alkyl phosphinic acids will help to further improve
9 the quantitative analysis of quantum dots (sizing curves and extinction coefficients). (3) CdSe
10 quantum dots synthesized with phosphinic acids fall into a size regime (2-3 nm) that is
11 traditionally difficult to access, especially for the wurtzite crystal structure.⁶³ The particles are
12 monodisperse and have a high photoluminescence quantum yield.
13
14
15
16
17
18
19
20
21
22
23
24
25
26

27 Although we have used here the cadmium chalcogenides as our model system to showcase the
28 versatility of mono-alkyl phosphinic acids, this ligand class is expected to be more widely
29 applicable in nanocrystal science. These ligands were indeed not designed for a specific
30 material. For example, unlike thiol ligands, they are expected to have also a good binding
31 affinity to metal oxide nanocrystals (e.g., ZrO₂), but this remains to be tested. Other open
32 questions concern the nucleation mechanism. It is striking that we easily found supporting
33 evidence for continuous nucleation in case of phosphonic acids and carboxylic acids but none
34 for phosphinic acids. Given that mono-alkyl phosphinic acids seems more well-behaved than
35 alkylphosphonic acids, mechanistic studies are more convenient and could tackle these open
36 questions.
37
38
39
40
41
42
43
44
45
46
47
48
49
50
51
52

53 **Conclusion**

54
55
56
57 We have presented convenient strategies to synthesize phosphinic acids that are relevant for
58 nanocrystals synthesis. Furthermore, cadmium phosphinate was shown to react with TOP-Se to
59
60

1
2
3 form CdSe nanocrystals of high purity, low polydispersity and reasonably high
4 photoluminescence quantum yield. We also demonstrated the synthesis of CdSe and CdS
5 nanorods with high shape uniformity for the latter. Compared to nanocrystals synthesized with
6 phosphonic acids, the ones synthesized with phosphinic acids are more easily purified since no
7 gel is formed. Interestingly, the reactivity of cadmium phosphinate is intermediate between
8 cadmium phosphonate and cadmium carboxylate. This provides researchers with an additional
9 handle on the kinetics of precursor conversion, which seems so far dominated by tuning the
10 chalcogen precursors. In addition, we did not find any indication of continuous nucleation in
11 the case of cadmium phosphinate. While this points to interesting mechanistic differences, more
12 detailed studies are necessary to uncover its wider implications.
13
14
15
16
17
18
19
20
21
22
23
24
25
26
27
28
29

30 **Experimental**

31
32
33
34 **General considerations.** All manipulations are performed in air, unless otherwise indicated.
35 All chemicals are used as received unless otherwise mentioned. *l*-Hexene (99%),
36 hypophosphorous acid (50% aqueous solution), lithium aluminium hydride (95%), potassium
37 hydrogen sulfate (99%), and triethylborane (1M in THF) were purchased from Acros. *l*-
38 Tetradecene (94%), cadmium oxide (99.998%), calcium hydride (92%), benzene (99.5%),
39 magnesium turnings (99.9%), magnesium sulfate (99.0%), sulfur (99.5%), and chloroform-d1
40 (99.8%D stabilized with Ag) were purchased from Carl Roth. Acetone (99%), acetonitrile
41 (99.9%), celite, chloroform (99.5%), dichloromethane (99.8%), diethyl ether (99.5%), dioxane
42 (99.9%), ethanol absolute (99.9%), ethyl acetate (99.5%), *n*-heptane (99%), *n*-hexane (99%),
43 hydrochloric acid (37%), methanol (99%), silica gel 60A (40-63 μm), sodium chloride (99.8%),
44 sodium hydroxide (98.5%), sodium sulfate (99%), tetrahydrofuran (99.9%), toluene (99.9%),
45 and trifluoroacetic acid (99%) were purchased from Chem-Lab. *n*-Hexylphosphonic acid
46
47
48
49
50
51
52
53
54
55
56
57
58
59
60

1
2
3 (97%), *n*-tetradecylphosphonic acid (97%), and *n*-octadecylphosphonic acid (97%) were
4 purchased from PlasmaChem. 1,2-Dibromoethane (98%), 1-bromooctadecane (97%), 1-
5 octadecene (90%), 1-octene (98%), 2-ethyl-hexylbromide (95%), benzoylperoxide (moistened
6 with 25% water), bromotrimethylsilane (97%), diethyl chlorophosphite (95%),
7 methanesulfonyl chloride (99.7%), oleic acid (90%), potassium carbonate (99%), potassium
8 hydroxide (90%), potassium *tert*-butoxide (98%), sodium hypophosphite monohydrate (99%)
9 tetrabromomethane (99%), trimethylamine (99%), and triphenylphosphine (99%) were
10 purchased from Sigma-Aldrich. Selenium (99.99%), tri-*n*-octylphosphine (90%), and tri-*n*-
11 octylphosphine oxide (90%) were purchased from STREM. Trifluoroacetic anhydride was
12 purchased from TCI. Benzene-*d*₆ (99.5%D), methanol-*d*₄ (99.8%D), and toluene-*d*₈ (99.5%D)
13 were purchased from VWR.

14
15
16
17
18
19
20
21
22
23
24
25
26
27
28
29 Some of the chemicals are toxic (*e.g.*, cadmium oxide), carcinogenic (*e.g.*, dichloromethane),⁸¹
30 or pyrophoric (*e.g.*, lithium aluminium hydride),⁸² and can have a severe impact on health and
31 environment on short and/or long term. It is advised to consult the available Safety Data Sheets
32 (SDS) provided by the producer prior to use. Specific safety consideration for NC synthesis
33 making use of TOPO and TOP have been described by Schaak *et al.* in more detail.⁸³

34
35
36
37
38
39
40
41
42 When required, organic solvents are dried according to the procedure described by Williams *et*
43 *al.*⁸⁴ making use of 20% m/v freshly activated 3Å sieves for minimum 120 hours.

44
45
46
47
48
49
50
51
52
53
54
55
56
57
58
59
60
61
62
63
64
65
66
67
68
69
70
71
72
73
74
75
76
77
78
79
80
81
82
83
84
85
86
87
88
89
90
91
92
93
94
95
96
97
98
99
100
101
102
103
104
105
106
107
108
109
110
111
112
113
114
115
116
117
118
119
120
121
122
123
124
125
126
127
128
129
130
131
132
133
134
135
136
137
138
139
140
141
142
143
144
145
146
147
148
149
150
151
152
153
154
155
156
157
158
159
160
161
162
163
164
165
166
167
168
169
170
171
172
173
174
175
176
177
178
179
180
181
182
183
184
185
186
187
188
189
190
191
192
193
194
195
196
197
198
199
200
201
202
203
204
205
206
207
208
209
210
211
212
213
214
215
216
217
218
219
220
221
222
223
224
225
226
227
228
229
230
231
232
233
234
235
236
237
238
239
240
241
242
243
244
245
246
247
248
249
250
251
252
253
254
255
256
257
258
259
260
261
262
263
264
265
266
267
268
269
270
271
272
273
274
275
276
277
278
279
280
281
282
283
284
285
286
287
288
289
290
291
292
293
294
295
296
297
298
299
300
301
302
303
304
305
306
307
308
309
310
311
312
313
314
315
316
317
318
319
320
321
322
323
324
325
326
327
328
329
330
331
332
333
334
335
336
337
338
339
340
341
342
343
344
345
346
347
348
349
350
351
352
353
354
355
356
357
358
359
360
361
362
363
364
365
366
367
368
369
370
371
372
373
374
375
376
377
378
379
380
381
382
383
384
385
386
387
388
389
390
391
392
393
394
395
396
397
398
399
400
401
402
403
404
405
406
407
408
409
410
411
412
413
414
415
416
417
418
419
420
421
422
423
424
425
426
427
428
429
430
431
432
433
434
435
436
437
438
439
440
441
442
443
444
445
446
447
448
449
450
451
452
453
454
455
456
457
458
459
460
461
462
463
464
465
466
467
468
469
470
471
472
473
474
475
476
477
478
479
480
481
482
483
484
485
486
487
488
489
490
491
492
493
494
495
496
497
498
499
500
501
502
503
504
505
506
507
508
509
510
511
512
513
514
515
516
517
518
519
520
521
522
523
524
525
526
527
528
529
530
531
532
533
534
535
536
537
538
539
540
541
542
543
544
545
546
547
548
549
550
551
552
553
554
555
556
557
558
559
560
561
562
563
564
565
566
567
568
569
570
571
572
573
574
575
576
577
578
579
580
581
582
583
584
585
586
587
588
589
590
591
592
593
594
595
596
597
598
599
600
601
602
603
604
605
606
607
608
609
610
611
612
613
614
615
616
617
618
619
620
621
622
623
624
625
626
627
628
629
630
631
632
633
634
635
636
637
638
639
640
641
642
643
644
645
646
647
648
649
650
651
652
653
654
655
656
657
658
659
660
661
662
663
664
665
666
667
668
669
670
671
672
673
674
675
676
677
678
679
680
681
682
683
684
685
686
687
688
689
690
691
692
693
694
695
696
697
698
699
700
701
702
703
704
705
706
707
708
709
710
711
712
713
714
715
716
717
718
719
720
721
722
723
724
725
726
727
728
729
730
731
732
733
734
735
736
737
738
739
740
741
742
743
744
745
746
747
748
749
750
751
752
753
754
755
756
757
758
759
760
761
762
763
764
765
766
767
768
769
770
771
772
773
774
775
776
777
778
779
780
781
782
783
784
785
786
787
788
789
790
791
792
793
794
795
796
797
798
799
800
801
802
803
804
805
806
807
808
809
810
811
812
813
814
815
816
817
818
819
820
821
822
823
824
825
826
827
828
829
830
831
832
833
834
835
836
837
838
839
840
841
842
843
844
845
846
847
848
849
850
851
852
853
854
855
856
857
858
859
860
861
862
863
864
865
866
867
868
869
870
871
872
873
874
875
876
877
878
879
880
881
882
883
884
885
886
887
888
889
890
891
892
893
894
895
896
897
898
899
900
901
902
903
904
905
906
907
908
909
910
911
912
913
914
915
916
917
918
919
920
921
922
923
924
925
926
927
928
929
930
931
932
933
934
935
936
937
938
939
940
941
942
943
944
945
946
947
948
949
950
951
952
953
954
955
956
957
958
959
960
961
962
963
964
965
966
967
968
969
970
971
972
973
974
975
976
977
978
979
980
981
982
983
984
985
986
987
988
989
990
991
992
993
994
995
996
997
998
999
1000

Trioctylphosphine oxide (TOPO) is recrystallized on a scale of 200 g by the procedure described by Owen *et al.* to obtain purified white needles (178 g, 89 %),^{27, 37} resulting in the same structure obtained by previous single-crystal XRD measurements.⁸⁵ Sulfur is recrystallized on a scale of 12.5 g by the following procedure. Sulfur is dissolved in toluene (1 mg/mL) at 100 °C and filtered over a hot frit. While the solution is cooling down to room temperature, shiny yellow needles grow. Afterwards, these needles are filtered and extensively

1
2
3 vacuum dried (9.0 g, 72 %). *n*-Octadecylphosphonic acid is synthesized according to the
4
5 procedure described by De Roo *et al.* on a 75 mmol *n*-octadecyl bromide scale (18.9 g, 76 %).²³
6

7 Di-*n*-octylphosphinic acid is synthesized according to the procedure described by Buhro *et al.*
8
9 on a 200 mmol hypophosphorous acid scale (17.2 g, 30 %).³⁷
10
11

12
13 **Synthesis of mono-alkylphosphinic acid.** Mono-alkylphosphinic acids are synthesized
14
15 according to the procedure of Montchamp *et al.* with slight adaptations.⁴⁸ An open 250 mL
16
17 flask is loaded with sodium hypophosphite hydrate (6.63 g, 62.5 mmol, 2.5 eq.), 1-alkene (25
18
19 mmol, 1.0 eq.), methanol (125 mL), and 1 mol L⁻¹ triethylborane in tetrahydrofuran (25 mL, 25
20
21 mmol, 1.0 eq.) which is vigorously stirred for 3 hours open to the air. Afterwards, the reaction
22
23 mixture is transferred to a separating funnel (1 L) to which dichloromethane (125 mL) and 1
24
25 mol L⁻¹ solution of KHSO₄ (125 mL) is added. The aqueous phase is washed once again with
26
27 dichloromethane (125 mL). All the organic phases are collected, dried with Na₂SO₄, and
28
29 concentrated on the rotary evaporator. For solid products, such as *n*-octadecyl- and *n*-
30
31 tetradecylphosphinic acid, a recrystallization from hot *n*-hexane (25 mL) is performed twice to
32
33 obtain a final purified white product. For liquid products, such as *n*-hexylphosphinic acid, the
34
35 product is first transformed to its potassium salt by adding a stoichiometric amount of potassium
36
37 hydroxide in EtOH (0.5 mol L⁻¹). After 1 hour stirring, the salt is concentrated on the rotary
38
39 evaporator and twice recrystallized from a hot mixture of *n*-hexane (10 mL), tetrahydrofuran
40
41 (10 mL), and ethanol (1 mL). The mixture is slowly cooled down to room temperature, fridge,
42
43 and overnight in the freezer (-20 °C). The precipitated product is filtered and collected. Purity
44
45 is checked using ³¹P NMR (if a residual peak at 3 ppm of hypophosphorous salt is observed, no
46
47 additional recrystallization is needed since it will get removed in the next washing step). To
48
49 obtain the final purified *n*-hexylphosphinic acid, the purified potassium *n*-hexylphosphinate salt
50
51 is acidified with conc. HCl (2 mL) in H₂O (5 ml) and extracted three times with
52
53 dichloromethane (5 mL). The organic fraction is collected and dried with Na₂SO₄, concentrated
54
55
56
57
58
59
60

1
2
3 on the rotary evaporator, and extensively vacuum dried. This reaction can be run at four times
4
5 the scale described with no observable changes.
6
7

8
9 *n-Octadecylphosphinic acid* (5.1 g, 61.0 %). $^1\text{H NMR}$ (300MHz, CDCl_3): δ 8.70 (s, 1H), 8.00
10
11 (t, $J = 1.8$ Hz, 0.5H), 6.20 (t, $J = 1.8$ Hz, 0.5H), 1.75 (quin, $J = 8.5$ Hz, 2H), 1.65-1.45 (m, 2H),
12
13 1.45-0.95 (m, 30H), 0.85 (t, $J = 7.0$ Hz, 3H). $^{13}\text{C NMR}$ (75MHz, CDCl_3): δ 32.10, 30.67, 30.50,
14
15 30.24, 29.87, 29.75, 29.53, 29.30, 28.99, 22.85, 20.62, 14.28. $^{31}\text{P}[1\text{H}] \text{NMR}$ (75MHz, CDCl_3):
16
17 δ 40.14 ppm. **LC-MS** (API-ES) calc for $\text{C}_{18}\text{H}_{38}\text{O}_2\text{P}$ $[\text{M}-\text{H}]^-$ 317.26, found 317.2.
18
19

20
21 *n-Tetradecylphosphinic acid* (3.2 g, 48.1 %). $^1\text{H NMR}$ (300MHz, CDCl_3): δ 9.45 (s, 1H), 8.00
22
23 (t, $J = 1.8$ Hz, 0.5H), 6.20 (t, $J = 1.8$ Hz, 0.5H), 1.75 (quin, $J = 8.5$ Hz, 2H), 1.60-1.35 (m, 2H),
24
25 1.35-0.95 (m, 22H), 0.85 (t, $J = 7.0$ Hz, 3H). $^{13}\text{C NMR}$ (75MHz, CDCl_3): δ 31.92, 30.52, 30.31,
26
27 30.02, 29.69, 29.66, 29.63, 29.59, 29.36, 29.13, 28.78, 22.69, 20.45, 14.11. $^{31}\text{P}[1\text{H}] \text{NMR}$
28
29 (75MHz, CDCl_3): δ 39.6 ppm. **LC-MS** (API-ES) calc for $\text{C}_{14}\text{H}_{32}\text{O}_2\text{P}$ $[\text{M}+\text{H}]^+$ 263.21, found
30
31 263.2.
32
33

34
35 *Potassium n-hexylphosphinate* (3.0 g, 63.2 %). $^1\text{H NMR}$ (300MHz, MeOD-d_4): δ 7.78 (t, $J =$
36
37 1.6 Hz, 0.5H), 6.16 (t, $J = 1.6$ Hz, 0.5H), 1.65-1.05 (m, 10H), 0.91 (t, $J = 6.9$ Hz, 3H). $^{13}\text{C NMR}$
38
39 (75MHz, MeOD-d_4): δ 34.37, 32.75, 31.79, 23.59, 23.05, 14.42. $^{31}\text{P}[1\text{H}] \text{NMR}$ (75MHz,
40
41 MeOD-d_4): δ 27.8 ppm. **LC-MS** (API-ES) calc for $\text{C}_6\text{H}_{10}\text{O}_2\text{PK}$ $[\text{M}-\text{K}]^-$ 149.07, found 149.2.
42
43
44

45
46 *n-Hexylphosphinic acid* (1.6 g, 42.0 %). $^1\text{H NMR}$ (300MHz, CDCl_3): δ 9.45 (s, 1H), 8.00 (t, J
47
48 = 1.8 Hz, 0.5H), 6.20 (t, $J = 1.8$ Hz, 0.5H), 1.75 (quin, $J = 8.5$ Hz, 2H), 1.65-1.45 (m, 2H), 1.35-
49
50 0.95 (m, 6H), 0.85 (t, $J = 7.0$ Hz, 3H). $^{13}\text{C NMR}$ (75MHz, CDCl_3): δ .31.40, 30.07, 28.64,
51
52 22.48, 20.67, 14.09. $^{31}\text{P}[1\text{H}] \text{NMR}$ (75MHz, CDCl_3): δ 38.7 ppm. **LC-MS** (API-ES) calc for
53
54 $\text{C}_6\text{H}_{16}\text{O}_2\text{P}$ $[\text{M}+\text{H}]^+$ 151.09, found 151.1.
55
56
57

58
59 **Synthesis of (Z)-octadec-9-en-1-ol (oleyl alcohol).** Oleyl alcohol is synthesized by reducing
60
oleic acid according to the procedure published by Grela *et al.*⁵⁰ In a 1 L flask, LiAlH_4 (10 g,

1
2
3 260 mmol, 3.5 eq.) is added, degassed three times, and put under argon. After the addition of
4
5 dry THF (300 mL), the flask is cooled to 0 °C in an ice bath. Dried oleic acid (21.48 g, 24.0
6
7 mL, 76 mmol, 1.0 eq.) is added dropwise. The reaction is allowed to heat up to room
8
9 temperature and stirred for 4 hours. Afterwards, the reaction flask is again cooled to 0 °C just
10
11 before diethyl ether (400 mL), H₂O (10 mL), 15% NaOH solution (10 mL), and H₂O (32 mL)
12
13 is carefully added. After 15 minutes of additional stirring, the reaction mixture is dried using
14
15 MgSO₄, and filtered over celite. The filtrate is first vacuum dried, and then vacuum distilled
16
17 following the same vacuum distillation procedure as described above to obtain a colourless
18
19 viscous liquid (17.5 g, 86 %). ¹H NMR (400MHz, CDCl₃): δ 5.40-5.25 (m, 2H), 3.60 (t, *J* =
20
21 6.6 Hz, 2H), 2.05-1.90 (m, 4H), 1.55 (quin, *J* = 7.0 Hz, 2H), 1.45 (s, 1H), 1.40-1.10 (m, 22H),
22
23 0.85 (t, *J* = 7.1 Hz, 3H). ¹³C NMR (75MHz, CDCl₃): δ 130.09, 129.94, 63.18, 32.93, 32.04,
24
25 29.90, 29.88, 29.66, 29.64, 29.55, 29.46, 29.37, 27.35, 27.33, 25.88, 22.82, 14.24. LC-MS
26
27 (API-ES) calc for C₁₈H₃₇O [M+H]⁺ 269.28, found 269.3.
28
29
30
31
32
33

34 **Synthesis of (*Z*)-octadec-9-en-1-yl methane sulfonate (oleyl mesylate).** In a 250 mL Schlenk
35
36 flask, oleyl alcohol (13.42 g, 15.51 mL, 50 mmol, 1.0 eq.) is added, degassed three times, and
37
38 put under argon. After the addition of dry dichloromethane (100 mL) and dried triethylamine
39
40 (5.57 g, 7.67 mL, 55 mmol, 1.1 eq.), the flask is cooled to 0 °C in an ice bath. Dry mesylate
41
42 chloride (6.30 g, 4.26 mL, 55 mmol, 1.1 eq.) is added dropwise and further stirred for 30
43
44 minutes, followed by the addition of H₂O (50 mL). After 30 minutes of additional stirring, the
45
46 reaction mixture is transferred to a separation funnel (300 mL) where the organic phase is kept
47
48 and the aqueous phase is extracted twice with chloroform (50 mL). All the organic phases are
49
50 collected together and washed with: (1) a mixture of 25% K₂CO₃ solution (25 mL) and H₂O
51
52 (50 mL); (2) brine (50 mL), and dried with MgSO₄. After vacuum drying, a colourless viscous
53
54 liquid is obtained (17.2 g, 99 %). ¹H NMR (300MHz, CDCl₃): δ 5.40-5.25 (m, 2H), 4.20 (t, *J*
55
56 = 6.6 Hz, 2H), 2.95 (s, 3H), 2.10-1.95 (m, 4H), 1.70 (quin, *J* = 7.5 Hz, 2H), 1.50-1.10 (m, 22H),
57
58
59
60

1
2
3 0.85 (t, $J = 7.2$ Hz, 3H). ^{13}C NMR (75MHz, CDCl_3): δ 130.18, 129.86, 70.30, 37.51, 32.05,
4
5 29.90, 29.83, 29.66, 29.46, 29.28, 29.15, 27.36, 27.30, 25.56, 22.82, 14.25. LC-MS (API-ES)
6
7 calc for $\text{C}_{19}\text{H}_{42}\text{NO}_3\text{S}$ $[\text{M}+\text{NH}_4]^+$ 364.29, found 364.3.
8
9

10
11 **Synthesis of (Z)-octadec-9-en-1-yl bromide (oleyl bromide).** Oleyl bromide is synthesized
12 according to the procedure of De Roo *et al.* with slight adaptations.²³ A 250 mL flask is loaded
13 with oleyl alcohol (13.42 g, 15.81 mL, 50 mmol, 1.0 eq.), tetrabromomethane (18.24 g, 55
14 mmol, 1.1 eq.), and dry dichloromethane (50 mL), and cooled to 0 °C with an ice bath.
15 Triphenylphosphine (15.74 g, 60 mmol, 1.2 eq.) was added in portions over 15 minutes. The
16 reaction was allowed to stir for 1 hour at room temperature. Afterwards, hexanes (50 mL) is
17 added to the mixture, cooled in the freezer to precipitate triphenylphosphine oxide, filtered over
18 a silica plug, and the filtrate is evaporated. This step is repeated a second time to remove all the
19 triphenylphosphine oxide, resulting in a colourless liquid (16.3 g, 98 %) which is vacuum dried
20 overnight to remove bromoform, and stored in fridge. ^1H NMR (300MHz, CDCl_3): δ 5.40-5.25
21 (m, 2H), 3.40 (t, $J = 6.9$ Hz, 2H), 2.10-1.90 (m, 4H), 1.85 (quin, $J = 7.7$ Hz, 2H), 1.50-1.10 (m,
22 22H), 0.85 (t, $J = 7.0$ Hz, 3H). ^{13}C NMR (75MHz, CDCl_3): δ 130.16, 129.91, 34.13, 33.01,
23 32.07, 29.94, 29.88, 29.70, 29.49, 29.35, 28.92, 28.35, 27.40, 27.33, 22.86, 14.28. GC-MS
24 molecular mass for $\text{C}_{18}\text{H}_{35}\text{Br}$ $[\text{M}]$ 331.38, found 331 (average mass).
25
26
27
28
29
30
31
32
33
34
35
36
37
38
39
40
41
42
43

44 **Synthesis of (Z)-octadeca-1,9-diene.** A 500 mL flask is loaded with oleyl bromide (16.57 g,
45 50 mmol, 1.0 eq.), evacuated, and set under argon atmosphere. Dry tetrahydrofuran (200 mL)
46 is added and cooled down to 0 °C with an ice bath. Potassium *tert*-butoxide (1M in THF, 115
47 mL, 115 mmol, 2.3 eq.) is added dropwise. It is important that a full yield is obtained since
48 separation between the diene and bromide is not straightforward. The reaction mixture is
49 allowed to warm to room temperature after the addition of the first equivalent of base and stirred
50 overnight. Afterwards, chloroform (200 mL) is added, and the mixture is washed twice with
51 water (200 mL) which is discarded. The organic phase is evaporated, and vacuum distilled over
52
53
54
55
56
57
58
59
60

1
2
3 CaH₂ to result in a colourless liquid (9.4 g, 75 %). **¹H NMR** (400MHz, CDCl₃): δ 5.90-5.70 (m,
4 1H), 5.40-5.25 (m, 2H), 5.05-4.85 (m, 2H), 2.10-1.90 (m, 6H), 1.50-1.15 (m, 20H), 0.85 (t, *J* =
5 7.1 Hz, 3H). **¹³C NMR** (75MHz, CDCl₃): δ 139.34, 130.12, 129.95, 114.29, 33.97, 32.08, 29.95,
6 29.89, 29.70, 29.50, 29.32, 29.20, 29.08, 27.40, 27.36, 22.87, 14.26. **GC-MS** molecular mass
7 for C₁₈H₃₄ [M] 250.47, found 250 (average mass).
8
9
10
11
12
13
14

15 **Synthesis of ethyl (2-ethylhexyl)phosphinate ester** according to the procedure of Meier *et*
16 *al.*⁵³ with slight adaptations. In an argon filled glovebox, a 250 mL Schlenk flask is loaded with
17 diethyl chlorophosphite (3913.8 mg, 3.595 mL, 25 mmol, 1.00 eq.) and dry tetrahydrofuran (50
18 mL). The flask is transferred to the Schlenk line and cooled down to 0 °C in an ice bath.
19 Separately, an oven dried 100 mL Schlenk flask is loaded with activated (sanded) magnesium
20 turnings (1.3 g, 52.5 mmol, 2.15 eq.), dry tetrahydrofuran (50 mL), 2-ethyl-hexylbromide
21 (3478.0 mg, 3.205 mL, 25 mmol, 1.00 eq.), a few drops of dry 1,2-dibromoethane, and is stirred
22 at room temperature overnight prior to a filtered Cannula transfer into the first solution. After
23 the addition, the reaction mixture is stirred overnight at 50 °C. The next day, the solvent is
24 evaporated, concentrated hydrochloric acid (5 mL) and water (75 mL) is added and stirred for
25 2 hours at room temperature. Afterwards, the reaction mixture is extracted twice with
26 dichloromethane (75 mL), dried with Na₂SO₄, concentrated on the rotary evaporator, and
27 purified using silica gel column chromatography (EtOAc). The final product is vacuum dried
28 overnight to remove all solvent traces and result in a colourless liquid (2.5 g, 49 %). **¹H NMR**
29 (400MHz, CDCl₃): δ 7.75 (t, *J* = 1.9 Hz, 0.5H), 6.45 (t, *J* = 2.1 Hz, 0.5H), 4.20-3.95 (m, 2H),
30 1.85-1.65 (m, 3H), 1.50-1.10 (m, 11H), 0.90-0.75 (m, 6H). **¹³C NMR** (100MHz, CDCl₃): δ
31 62.40, 33.89, 33.54, 32.65, 28.57, 27.14, 22.90, 16.34, 14.11, 10.57. **³¹P[¹H] NMR** (160MHz,
32 CDCl₃): δ 38.53 ppm. **LC-MS** (API-ES) calc for C₁₀H₂₄O₂P [M+H]⁺ 207.15, found 207.2.
33
34
35
36
37
38
39
40
41
42
43
44
45
46
47
48
49
50
51
52
53
54
55
56
57

58 **Synthesis of ethyl (oleyl)phosphinate ester** is synthesized using the same procedure as for
59 ethyl (2-ethylhexyl)phosphinate ester but with oleyl bromide (8284.3 mg, 25 mmol, 1.00 eq.)
60

1
2
3 instead of 2-ethyl-hexylbromide. The final product is a colourless liquid (1.6 g, 18.6 %). **¹H**
4 **NMR** (400MHz, CDCl₃): δ 7.70 (t, *J* = 1.8 Hz, 0.5H), 6.40 (t, *J* = 1.9 Hz, 0.5H), 5.40-5.25 (m,
5 2H), 4.25-3.95 (m, 2H), 2.10-1.85 (m, 4H), 1.80-1.65 (m, 2H), 1.65-1.50 (m, 2H), 1.50-1.15
6 (m, 25H), 0.85 (t, *J* = 6.8 Hz, 3H). **¹³C NMR** (100MHz, CDCl₃): δ 130.12, 129.84, 62.38, 32.02,
7 30.63, 30.48, 29.89, 29.80, 29.65, 29.44, 29.37, 29.31, 29.24, 28.42, 27.37, 27.28, 22.79, 20.84,
8 16.40, 14.22. **³¹P[¹H] NMR** (160MHz, CDCl₃): δ 38.94 ppm. **LC-MS** (API-ES) calc for
9 C₂₀H₄₂O₂P [M+H]⁺ 345.29, found 345.3.

10
11
12
13
14
15
16
17
18
19
20 **Synthesis of 2-ethylhexyl and oleylphosphinic acid.** The phosphinate is dissolved in dry
21 dichloromethane (2 mL per gram phosphinate) in dried Schlenk flask. TMS-Br (1.15
22 equivalents) is added and the reaction mixture is stirred overnight under argon. The volatiles
23 are removed by evaporation, excess dry methanol (5 mL per gram phosphinate) is added and
24 the solution is stirred for 6 hours at 40 °C. Afterwards, the solvent is removed by evaporation
25 and the product is vacuum dried overnight at 50 °C to remove methanol.

26
27
28
29
30
31
32
33
34
35 *2-Ethylhexylphosphinic acid, quantitative yield.* **¹H NMR** (400MHz, CDCl₃): δ 11.50 (s, 1H)
36 7.85 (s, 0.5H), 6.50 (s, 0.5H), 1.90-1.65 (m, 3H), 1.55-1.10 (m, 8H), 0.95-0.75 (m, 6H). **¹³C**
37 **NMR** (100MHz, CDCl₃): δ 33.90, 33.81, 33.36, 28.53, 27.10, 22.93, 14.16, 10.52. **³¹P[¹H]**
38 **NMR** (160MHz, CDCl₃): δ 38.29 ppm. **LC-MS** (API-ES) calc for C₈H₂₀O₂P [M+H]⁺ 179.12,
39 found 179.2.

40
41
42
43
44
45
46
47
48
49
50
51
52
53
54
55
56
57
58
59
60 *Oleylphosphinic acid, quantitative yield.* **¹H NMR** (400MHz, CDCl₃): δ 11.50 (s, 1H), 7.75 (s,
0.5H), 6.40 (s, 0.5H), 5.40-5.25 (m, 2H), 2.10-1.85 (m, 4H), 1.85-1.65 (m, 2H), 1.65-1.50 (m,
2H), 1.50-1.15 (m, 22H), 0.85 (t, *J* = 7.0 Hz, 3H). **¹³C NMR** (100MHz, CDCl₃): δ 130.14,
129.88, 32.07, 30.64, 30.49, 29.93, 29.87, 29.68, 29.47, 29.42, 29.38, 29.26, 28.94, 27.38,
27.32, 22.83, 20.71, 14.27. **³¹P[¹H] NMR** (160MHz, CDCl₃): δ 38.83 ppm. **LC-MS** (API-ES)
calc for C₁₈H₃₆O₂P [M-H]⁻ 315.25, found 135.2.

1
2
3 **Synthesis of cadmium *n*-tetradecylphosphinate.** The procedure is inspired by the one used
4 to synthesize cadmium oleate of Hendricks *et al.*^{15-16, 86} CdO (642.1 mg, 5 mmol, 1 eq.) and
5 acetonitrile (4 mL) are stirred at 0 °C in an ice bath. Trifluoroacetic anhydride (708 μL, 5 mmol,
6 1 eq.) and trifluoroacetic acid (77 μL, 1 mmol, 0.2 eq.) are added and allowed to warm to room
7 temperature and results in a clear and colourless solution overnight, (if the resulting solution
8 would have a white precipitate, a little more acetonitrile or heat results in a clear and colourless
9 solution). This solution is added dropwise to a mixture of *n*-tetradecylphosphinic acid (2636.8
10 mg, 10.05 mmol, 2.1 eq.) and triethylamine (1143.5 mg, 11.3 mmol, 2.25 eq.) in
11 dichloromethane (20 mL). The reaction mixture is heated to reflux for an hour. Afterwards, the
12 flask is slowly cooled to room temperature and then put in a freezer. The resulting white powder
13 is filtered on a glass frit and carefully washed by going through the slurry and break-up large
14 chunks three times with cold methanol (40 mL). The final product is vacuum dried and yields
15 a fine white powder (4.7 g, 93 %). **Elemental analysis** (CHNS) calc for C₂₈H₆₀O₄P₂Cd: %C
16 52.95, %H 9.54, %N 0.00, %S 0.00; found %C 51.78, %H 9.78, %N 0.49, %S 0.00.
17
18
19
20
21
22
23
24
25
26
27
28
29
30
31
32
33
34
35

36 **Synthesis of cadmium selenide (CdSe) quantum dots according to Owen *et al.***²⁷ A 50 mL
37 three neck flask, equipped with a small reflux condenser and silicon/PTFE septum, is loaded
38 with cadmium oxide (172.1 mg, 1.34 mmol, 1.12 eq.), *n*-octadecylphosphonic acid (752.6 mg,
39 2.7 mmol, 2.25 eq.), and TOPO (15.0 g). The mixture is degassed (evacuated) for 30 minutes
40 at 100 °C. The flask is filled with argon and heated to 330 °C until the CdO digests into a
41 colourless solution. Afterwards, the temperature is lowered to 300 °C at which point 1.3 mL
42 (1065.0 mg, 1.2 mmol, 1.00 eq.) of a premade TOP-Se solution (4.5 mmol Se per 4 gram TOP
43 prepared stirring overnight in an argon filled glovebox) is rapidly injected. After the preferred
44 reaction time, the mixture is cooled down to 60 °C at which point the reaction mixture is divided
45 equally into 2 centrifuge tubes (50 mL) and the QDs are purified 3 times by precipitation with
46 acetone (40 mL) and redispersion in toluene (5 mL) after centrifugation (10k rpm, 10 minutes).
47
48
49
50
51
52
53
54
55
56
57
58
59
60

1
2
3 For the synthesis with phosphinic acid or carboxylic acid, we simply replaced *n*-
4 octadecylphosphonic acid by *n*-octadecylphosphinic acid (752.6 mg, 2.7 mmol, 2.25 eq.) or
5 oleic acid (762.7 mg, 0.852 mL, 2.70 mmol, 2.25 eq.) respectively. Since the acidity of the
6 phosphinic and carboxylic acid is slightly lower compared to the phosphonic acid, CdO is
7 digested at a higher temperature (375 °C) for 4 hours until the colour of the mixture evolved
8 into almost transparent/white suspension.
9

10
11
12 **Synthesis of cadmium selenide (CdSe) nanorods according Buhro *et al.*³⁶** A 25 mL three
13 neck flask is loaded with cadmium oxide (51.4 mg, 0.4 mmol, 1.0 eq.), di-*n*-octylphosphinic
14 acid (203.3 mg, 0.7 mmol, 1.75 eq.), *n*-tetradecylphosphonic acid (222.7 mg, 0.8 mmol, 2.0
15 eq.), and TOPO (3.8g). The mixture is degassed for 40 minutes at 120 °C. The flask is filled
16 with argon and heated to 320 °C until the CdO digests into a colourless solution. Afterwards,
17 the temperature is lowered to 150 °C for a second degassing step for 1 hour. The flask is filled
18 with argon and heated to 275 °C, at which point 1.2 mL of a premade TOP-Se solution (3.0
19 mmol Se per 5 g TOP prepared stirring overnight in an argon filled glovebox) is rapidly injected.
20 After 30 minutes, the reaction is cooled down to 60 °C at which point the reaction mixture is
21 transferred to a centrifuge tube (50 mL) and the NRs are purified 3 times by precipitation with
22 acetone (40 mL) and redispersion in toluene (5mL) after centrifugation (10k rpm, 10 minutes).
23
24

25
26
27 For the synthesis with phosphinic acid, we replaced CdO and *n*-tetradecylphosphonic acid by
28 presynthesized Cd(*n*-tetradecylphosphinate)₂ (254.1 mg, 0.4 mmol, 1.00 eq.). Since the
29 phosphinic acids (*n*-tetradecyl and di-*n*-octyl) have a similar acidity they both digest the CdO
30 resulting in a white turbid suspension.
31
32

33
34
35 **Cadmium sulfide (CdS) NRs adapted Buhro *et al.*³⁶** Here the same recipe is followed as for
36 the CdSe NRs but where TOP-Se is replaced by TOP-S (3.0 mmol S per 5 gram TOP).
37
38
39
40
41
42
43
44
45
46
47
48
49
50
51
52
53
54
55
56
57
58
59
60

1
2
3 For the synthesis with phosphinic acid, we replaced CdO and *n*-tetradecylphosphonic acid by
4 presynthesized Cd(*n*-tetradecylphosphinate)₂ (254.1 mg, 0.4 mmol, 1.00 eq.) with a reaction
5
6 time of 1 hour, all other parameters remained identical.
7
8
9

10
11 **Electron Microscopy.** Transmission Electron Microscopy (TEM) and High-Resolution
12 Transmission Electron Microscopy (HRTEM) were performed on a JEOL JEM-2200FS TEM
13 with Cs corrector operated at 200 kV (bright field).
14
15
16

17
18 **Size and Concentration Determination.** The optical band gaps of the NCs were determined
19 by UV–vis–NIR absorption spectroscopy (PerkinElmer Lambda 950). Aliquots of
20 approximately 0.1 mL were taken from a CdSe or CdS nanocrystal reaction and deposited into
21 a previously weighed vial with 3 mL of hexane. Afterwards, the mixture was further diluted to
22 obtain 10 mg mL⁻¹ reaction mixture solutions in hexane. UV-Vis absorption spectra were taken
23 of each aliquot and the concentration of cadmium selenide in the aliquot was calculated from
24 the size-independent absorption coefficient for CdSe at 340 nm ($\mu = 141100 \text{ cm}^{-1}$) reported by
25 Capek *et al.*⁵⁸ The size of the NCs was determined from the position of the first excitonic
26 absorption peak using the sizing curve described by Maes *et al.*⁸⁷
27
28
29
30
31
32
33
34
35
36
37
38
39

40 **NMR Spectroscopy.** Nuclear Magnetic Resonance (NMR) spectra of the synthesized organics
41 were recorded on a Bruker 300, and 400 MHz. Chemical shifts (δ) are given in ppm and the
42 residual solvent peak was used as an internal standard (CDCl₃: $\delta\text{H} = 7.24 \text{ ppm}$, $\delta\text{C} = 77.06$
43 ppm, CD₃OD: $\delta\text{H} = 3.31 \text{ ppm}$, $\delta\text{C} = 49.00 \text{ ppm}$, C₆D₆: $\delta\text{H} = 7.16 \text{ ppm}$, $\delta\text{C} = 128.06 \text{ ppm}$,
44 toluene-*d*₈: $\delta\text{H} = 2.09 \text{ ppm}$, $\delta\text{C} = 20.43 \text{ ppm}$, C₆D₆: $\delta\text{H} = 7.16 \text{ ppm}$, $\delta\text{C} = 128.06 \text{ ppm}$). The
45 signal multiplicity is denoted as follows: s (singlet), d (doublet), t (triplet), quad (quadruplet),
46 quin (quintet), m (multiplet). Coupling constants are reported in Hertz (Hz). ¹H and ¹³C spectra
47 were acquired using the standard pulse sequences from the Bruker library; zg30 and jmod
48 (Attached Proton Test = APT) In the APT, the carbon resonances resulting from a -CH₂- and
49 quaternary -C_q- are “in-phase” (orientated up), whereas the carbon resonances resulting from a
50
51
52
53
54
55
56
57
58
59
60

1
2
3 -CH₃- or -CH- are “out-of-phase” (orientated down). Although one could easily reverse the
4
5 phase 180° and achieve the inverse result. ³¹P spectra of organic compounds were acquired with
6
7 proton decoupling (zgpg30) and a relaxation delay (= recycle delay, or D1) of 2 seconds. All
8
9 resonances were corrected prior to integration by subtracting a background from the measured
10
11 intensity. The chemical shifts for other nuclei were referenced indirectly to the ¹H NMR
12
13 frequency of the sample with the ‘xiref’-macro in Bruker.
14
15

16
17 Nuclear Magnetic Resonance (NMR) measurements of colloidal nanocrystals were recorded on
18
19 a Bruker Avance III Spectrometer operating at a ¹H frequency of 500.13 MHz and featuring a
20
21 BBI probe. The sample temperature was set to 298.15. For the quantitative 1D ¹H
22
23 measurements, 64k data points were sampled with the spectral width set to 16 ppm and a
24
25 relaxation delay (= recycle delay, or D1) of 30 seconds to allow full relaxation of all NMR
26
27 signals. The quantification was done by using the Digital ERETIC method.⁸⁸⁻⁸⁹ One-
28
29 dimensional ³¹P spectra of nanocrystals were acquired using the standard pulse sequence
30
31 zgpgseig from the Bruker library (with a tau echo delay, *i.e.* D16 =200 μs, and a relaxation
32
33 delay (D1) of 2 seconds). DOSY measurements were performed with a double stimulated echo
34
35 pulses (dstegp3s) for convection compensation and with monopolar gradient pulses,⁹⁰ and a
36
37 relaxation delay (D1) of 1 second. The gradient strength was varied quadratically from 2-95%
38
39 of the probe’s maximum value in 64 steps, with the pulse length gradient (D20) and diffusion
40
41 time (P30) optimized to ensure a final attenuation of the signal in the final increment of less
42
43 than 8% relative to the first increment.
44
45
46
47
48
49

50 **X-ray total scattering experiments.** The samples were loaded in 1 mm polyimide tubes. The
51
52 X-ray total scattering experiments were performed at beamline P02.1, DESY, Hamburg,
53
54 Germany in rapid acquisition geometry, using a 2D detector (150 × 150 μm pixel size) with a
55
56 sample to detector distance of 268 mm. The incident wavelength of the X-rays was $\lambda = 0.2073$
57
58 Å (59.8 keV). Calibration of the experimental setup was performed using a CeO₂ standard. Raw
59
60

1
2
3 2D data were corrected for geometrical effects and polarization, then azimuthally integrated to
4
5 produce 1D scattering intensities versus the magnitude of the momentum transfer Q (where Q
6
7 $= 4\pi \sin \theta/\lambda$ for elastic scattering) using Dioptas.⁹¹ xPDFsuite with PDFgetX3 was used to
8
9 perform the background subtraction, further corrections, and normalization to obtain the
10
11 reduced total scattering structure function $F(Q)$, and Fourier transformation to obtain the pair
12
13 distribution function (PDF), $G(r)$.⁹²⁻⁹³ The following parameters were used for data reduction:
14
15 $Q_{\min} = 0.8 \text{ \AA}^{-1}$, $Q_{\max} = 17.5 \text{ \AA}^{-1}$, $Q_{\text{inst}} = 17.5 \text{ \AA}^{-1}$ and $R_{\text{poly}} = 0.9 \text{ \AA}$. Modeling and fitting was
16
17 done using Diffpy-CMI.⁹⁴
18
19
20
21

22 **Photoluminescence.** Photoluminescence spectra were measured upon excitation with a fiber
23
24 coupled LED (20mA) having an emission peak wavelength of 400 nm. The samples were
25
26 measured in a Spectralon coated integrating sphere. The emission spectra were analyzed with a
27
28 fiber coupled Acton SP2300 monochromator and detected by a ProEM 1600 EMCCD
29
30 (Princeton Instruments). The spectra were properly corrected for the spectral sensitivity of the
31
32 detector part. The PLQY values were calculated by dividing the integrated number of emitted
33
34 photons by the number of absorbed photons upon excitation.
35
36
37
38

39 **Mass spectroscopy.** Mass spectra (MS) are measured with an Agilent ESI single quadrupole
40
41 detector type VL and an Agilent APCI single quadrupole detector type VL.
42
43
44

45 **Elemental Analysis.** A Thermo Scientific Flash 2000 CHNS-O analyzer equipped with a TCD
46
47 detector was used to perform elemental analysis (C/H/N).
48
49

50 **FTIR spectroscopy.** Infrared spectra (IR) are recorded with a Perkin-Elmer Spectrum1000
51
52 FTIR Infrared Spectrometer.
53
54
55
56
57
58
59

60 **Acknowledgements**

1
2
3 The authors acknowledge the FWO Vlaanderen (1S28818N), Special Research Fund/Concerted
4 Research Actions project (BOF2015/GOA/007), Ghent University, and Basel University for
5 financial support. The authors thank Jan Goeman for the GC/LC-MS, and Funda Aliç for
6 elemental analysis. The authors acknowledge funding from the Danish Ministry of Higher
7 Education and Science through the SMART Lighthouse. The authors thank DANSCATT
8 (supported by the Danish Agency for Science and Higher Education) for support. The authors
9 acknowledge DESY (Hamburg, Germany), a member of the Helmholtz Association HGF, for
10 the provision of experimental facilities. Parts of this research were carried out at P02.1 and the
11 authors thank Martin Etter for assistance in using the beamline.
12
13
14
15
16
17
18
19
20
21
22
23
24
25
26
27

28 **Associated Content**

29 **Supporting information**

30
31
32 Provides additional HR-TEM, PDF data and results, detailed results of various experiments, ¹H
33 NMR of surface chemistry, UV-Vis absorption spectra, PLQY spectra, and NMR spectra of
34 synthesized compounds. This material is available free of charge via the Internet at
35 <http://pubs.acs.org/>.
36
37
38
39
40
41
42
43
44

45 **Preprint version**

46
47
48 Evert Dhaene, Philippe F. Smet, Klaartje De Buysser, Jonathan De Roo, Mono-alkyl
49 Phosphinic Acids as Ligands in Nanocrystal Synthesis. 2021, 10.26434/chemrxiv-2021-0hw9k.
50 ChemRxiv. <https://chemrxiv.org/engage/chemrxiv/article-details/6127992c8e38a370e5412bc9>
51 (accessed April 19, 2022).
52
53
54
55
56
57
58
59
60

Author Information

Corresponding Author

*E-mail: Jonathan.DeRoo@unibas.ch

ORCID

Evert Dhaene: 0000-0002-1604-0408

Rohan Pokratath: 0000-0002-6838-3939

Olivia Aalling-Frederiksen: 0000-0003-1462-7173

Kirsten M. Ø. Jensen: 0000-0003-0291-217X

Philippe F. Smet: 0000-0003-4789-5799

Klaartje De Buysser: 0000-0001-7462-2484

Jonathan De Roo: 0000-0002-1264-9312

Notes

The authors declare no competing financial interest.

References

1. Nanomaterials Definition Matters. *Nature Nanotechnology* **2019**, *14* (3), 193-193.
2. Boles, M. A.; Ling, D.; Hyeon, T.; Talapin, D. V., The Surface Science of Nanocrystals. *Nature Materials* **2016**, *15* (2), 141-153.
3. Yang, Y.; Qin, H.; Jiang, M.; Lin, L.; Fu, T.; Dai, X.; Zhang, Z.; Niu, Y.; Cao, H.; Jin, Y.; Zhao, F.; Peng, X., Entropic Ligands for Nanocrystals: From Unexpected Solution Properties to Outstanding Processability. *Nano Letters* **2016**, *16* (4), 2133-2138.
4. Yang, Y.; Qin, H.; Peng, X., Intramolecular Entropy and Size-Dependent Solution Properties of Nanocrystal–Ligands Complexes. *Nano Letters* **2016**, *16* (4), 2127-2132.

5. Doblas, D.; Kister, T.; Cano-Bonilla, M.; González-García, L.; Kraus, T., Colloidal Solubility and Agglomeration of Apolar Nanoparticles in Different Solvents. *Nano Letters* **2019**, *19* (8), 5246-5252.
6. Kister, T.; Monego, D.; Mulvaney, P.; Widmer-Cooper, A.; Kraus, T., Colloidal Stability of Apolar Nanoparticles: The Role of Particle Size and Ligand Shell Structure. *ACS Nano* **2018**, *12* (6), 5969-5977.
7. Monego, D.; Kister, T.; Kirkwood, N.; Doblas, D.; Mulvaney, P.; Kraus, T.; Widmer-Cooper, A., When Like Destabilizes Like: Inverted Solvent Effects in Apolar Nanoparticle Dispersions. *ACS Nano* **2020**, *14* (5), 5278-5287.
8. Monego, D.; Kister, T.; Kirkwood, N.; Mulvaney, P.; Widmer-Cooper, A.; Kraus, T., Colloidal Stability of Apolar Nanoparticles: Role of Ligand Length. *Langmuir* **2018**, *34* (43), 12982-12989.
9. Heuer-Jungemann, A.; Feliu, N.; Bakaimi, I.; Hamaly, M.; Alkilany, A.; Chakraborty, I.; Masood, A.; Casula, M. F.; Kostopoulou, A.; Oh, E.; Susumu, K.; Stewart, M. H.; Medintz, I. L.; Stratakis, E.; Parak, W. J.; Kanaras, A. G., The Role of Ligands in the Chemical Synthesis and Applications of Inorganic Nanoparticles. *Chemical Reviews* **2019**, *119* (8), 4819-4880.
10. Mozaffari, S.; Li, W.; Thompson, C.; Ivanov, S.; Seifert, S.; Lee, B.; Kovarik, L.; Karim, A. M., Colloidal Nanoparticle Size Control: Experimental and Kinetic Modeling Investigation of the Ligand–Metal Binding Role in Controlling the Nucleation and Growth Kinetics. *Nanoscale* **2017**, *9* (36), 13772-13785.
11. Abe, S.; Capek, R. K.; De Geyter, B.; Hens, Z., Reaction Chemistry/Nanocrystal Property Relations in the Hot Injection Synthesis, the Role of the Solute Solubility. *ACS Nano* **2013**, *7* (2), 943-949.
12. Peters, E. H.; Mayor, M., Monofunctionalized Gold Nanoparticles: Fabrication and Applications. *Chimia* **2021**, *75* (5), 414-426.
13. Knauf, R. R.; Lennox, J. C.; Dempsey, J. L., Quantifying Ligand Exchange Reactions at CdSe Nanocrystal Surfaces. *Chemistry of Materials* **2016**, *28* (13), 4762-4770.
14. Li, L.; Daou, T. J.; Texier, I.; Kim Chi, T. T.; Liem, N. Q.; Reiss, P., Highly Luminescent CuInS₂/ZnS Core/Shell Nanocrystals: Cadmium-Free Quantum Dots for *In Vivo* Imaging. *Chemistry of Materials* **2009**, *21* (12), 2422-2429.
15. Hendricks, M. P.; Campos, M. P.; Cleveland, G. T.; Jen-La Plante, I.; Owen, J. S., A tunable library of substituted thiourea precursors to metal sulfide nanocrystals. *Science* **2015**, *348* (6240), 1226-1230.
16. Hamachi, L. S.; Jen-La Plante, I.; Coryell, A. C.; De Roo, J.; Owen, J. S., Kinetic Control over CdS Nanocrystal Nucleation Using a Library of Thiocarbonates, Thiocarbamates, and Thioureas. *Chemistry of Materials* **2017**, *29* (20), 8711-8719.
17. Park, J.; An, K.; Hwang, Y.; Park, J.-G.; Noh, H.-J.; Kim, J.-Y.; Park, J.-H.; Hwang, N.-M.; Hyeon, T., Ultra-Large-Scale Syntheses of Monodisperse Nanocrystals. *Nature Materials* **2004**, *3* (12), 891-895.
18. García-Rodríguez, R.; Hendricks, M. P.; Cossairt, B. M.; Liu, H.; Owen, J. S., Conversion Reactions of Cadmium Chalcogenide Nanocrystal Precursors. *Chemistry of Materials* **2013**, *25* (8), 1233-1249.
19. De Roo, J.; De Keukeleere, K.; Hens, Z.; Van Driessche, I., From Ligands to Binding Motifs and Beyond; the Enhanced Versatility of Nanocrystal Surfaces. *Dalton Transactions* **2016**, *45* (34), 13277-13283.
20. Leemans, J.; Dümbgen, K. C.; Minjauw, M. M.; Zhao, Q.; Vantomme, A.; Infante, I.; Detavernier, C.; Hens, Z., Acid–Base Mediated Ligand Exchange on Near-Infrared Absorbing, Indium-Based III–V Colloidal Quantum Dots. *Journal of the American Chemical Society* **2021**, *143* (11), 4290-4301.
21. Oliva-Puigdomènech, A.; De Roo, J.; Kuhs, J.; Detavernier, C.; Martins, J. C.; Hens, Z., Ligand Binding to Copper Nanocrystals: Amines and Carboxylic Acids and the Role of Surface Oxides. *Chemistry of Materials* **2019**, *31* (6), 2058-2067.
22. Gomes, R.; Hassinen, A.; Szczygiel, A.; Zhao, Q.; Vantomme, A.; Martins, J. C.; Hens, Z., Binding of Phosphonic Acids to CdSe Quantum Dots: A Solution NMR Study. *The Journal of Physical Chemistry Letters* **2011**, *2* (3), 145-152.
23. De Roo, J.; Zhou, Z.; Wang, J.; Deblock, L.; Crosby, A. J.; Owen, J. S.; Nonnenmann, S. S., Synthesis of Phosphonic Acid Ligands for Nanocrystal Surface Functionalization and Solution Processed Memristors. *Chemistry of Materials* **2018**, *30* (21), 8034-8039.

- 1
2
3 24. De Roo, J.; Huang, Z.; Schuster, N. J.; Hamachi, L. S.; Congreve, D. N.; Xu, Z.; Xia, P.; Fishman, D.
4 A.; Lian, T.; Owen, J. S.; Tang, M. L., Anthracene Diphosphate Ligands for CdSe Quantum Dots;
5 Molecular Design for Efficient Upconversion. *Chemistry of Materials* **2020**, *32* (4), 1461-1466.
- 6 25. Nemat, S. J.; Van den Eynden, D.; Deblock, L.; Heilmann, M.; Köster, J. M.; Parvizian, M.;
7 Tiefenbacher, K.; De Roo, J., Resorcin[4]arene-Based Multidentate Phosphate Ligands with Superior
8 Binding Affinity for Nanocrystal Surfaces. *Chemical Communications* **2021**, *57* (38), 4694-4697.
- 9 26. Peng, Z. A.; Peng, X., Formation of High-Quality CdTe, CdSe, and CdS Nanocrystals Using CdO
10 as Precursor. *Journal of the American Chemical Society* **2001**, *123* (1), 183-184.
- 11 27. Owen, J. S.; Park, J.; Trudeau, P.-E.; Alivisatos, A. P., Reaction Chemistry and Ligand Exchange
12 at Cadmium–Selenide Nanocrystal Surfaces. *Journal of the American Chemical Society* **2008**, *130* (37),
13 12279-12281.
- 14 28. Carbone, L.; Nobile, C.; De Giorgi, M.; Sala, F. D.; Morello, G.; Pompa, P.; Hytch, M.; Snoeck, E.;
15 Fiore, A.; Franchini, I. R.; Nadasan, M.; Silvestre, A. F.; Chiodo, L.; Kudera, S.; Cingolani, R.; Krahne, R.;
16 Manna, L., Synthesis and Micrometer-Scale Assembly of Colloidal CdSe/CdS Nanorods Prepared by a
17 Seeded Growth Approach. *Nano Letters* **2007**, *7* (10), 2942-2950.
- 18 29. Zhang, B.; Goldoni, L.; Zito, J.; Dang, Z.; Almeida, G.; Zaccaria, F.; de Wit, J.; Infante, I.; De Trizio,
19 L.; Manna, L., Alkyl Phosphonic Acids Deliver CsPbBr₃ Nanocrystals with High Photoluminescence
20 Quantum Yield and Truncated Octahedron Shape. *Chemistry of Materials* **2019**, *31* (21), 9140-9147.
- 21 30. Zhang, B.; Goldoni, L.; Lambruschini, C.; Moni, L.; Imran, M.; Pianetti, A.; Pinchetti, V.; Brovelli,
22 S.; De Trizio, L.; Manna, L., Stable and Size Tunable CsPbBr₃ Nanocrystals Synthesized with
23 Oleylphosphonic Acid. *Nano Letters* **2020**, *20* (12), 8847-8853.
- 24 31. Drijvers, E.; De Roo, J.; Geiregat, P.; Fehér, K.; Hens, Z.; Aubert, T., Revisited Wurtzite CdSe
25 Synthesis: A Gateway for the Versatile Flash Synthesis of Multishell Quantum Dots and Rods. *Chemistry
26 of Materials* **2016**, *28* (20), 7311-7323.
- 27 32. Liu, H.; Owen, J. S.; Alivisatos, A. P., Mechanistic Study of Precursor Evolution in Colloidal Group
28 II–VI Semiconductor Nanocrystal Synthesis. *Journal of the American Chemical Society* **2007**, *129* (2),
29 305-312.
- 30 33. Owen, J. S.; Chan, E. M.; Liu, H.; Alivisatos, A. P., Precursor Conversion Kinetics and the
31 Nucleation of Cadmium Selenide Nanocrystals. *Journal of the American Chemical Society* **2010**, *132*
32 (51), 18206-18213.
- 33 34. De Keukeleere, K.; Coucke, S.; De Canck, E.; Van Der Voort, P.; Delpech, F.; Coppel, Y.; Hens, Z.;
34 Van Driessche, I.; Owen, J. S.; De Roo, J., Stabilization of Colloidal Ti, Zr, and Hf Oxide Nanocrystals by
35 Protonated Tri-n-octylphosphine Oxide (TOPO) and Its Decomposition Products. *Chemistry of
36 Materials* **2017**, *29* (23), 10233-10242.
- 37 35. Wolcott, A.; Fitzmorris, R. C.; Muzaffery, O.; Zhang, J. Z., CdSe Quantum Rod Formation Aided
38 By In Situ TOPO Oxidation. *Chemistry of Materials* **2010**, *22* (9), 2814-2821.
- 39 36. Wang, F.; Buhro, W. E., Morphology Control of Cadmium Selenide Nanocrystals: Insights into
40 the Roles of Di-n-octylphosphine Oxide (DOPO) and Di-n-octylphosphinic Acid (DOPA). *Journal of the
41 American Chemical Society* **2012**, *134* (11), 5369-5380.
- 42 37. Wang, F.; Tang, R.; Buhro, W. E., The Trouble with TOPO; Identification of Adventitious
43 Impurities Beneficial to the Growth of Cadmium Selenide Quantum Dots, Rods, and Wires. *Nano
44 Letters* **2008**, *8* (10), 3521-3524.
- 45 38. Wang, F.; Tang, R.; Kao, J. L. F.; Dingman, S. D.; Buhro, W. E., Spectroscopic Identification of Tri-
46 n-octylphosphine Oxide (TOPO) Impurities and Elucidation of Their Roles in Cadmium Selenide
47 Quantum-Wire Growth. *Journal of the American Chemical Society* **2009**, *131* (13), 4983-4994.
- 48 39. Kloda, M.; Ondrušová, S.; Lang, K.; Demel, J., Phosphinic Acids as Building Units in Materials
49 Chemistry. *Coordination Chemistry Reviews* **2021**, *433*, 213748.
- 50 40. Jasieniak, J.; Bullen, C.; van Embden, J.; Mulvaney, P., Phosphine-Free Synthesis of CdSe
51 Nanocrystals. *The Journal of Physical Chemistry B* **2005**, *109* (44), 20665-20668.
- 52 41. van Embden, J.; Mulvaney, P., Nucleation and Growth of CdSe Nanocrystals in a Binary Ligand
53 System. *Langmuir* **2005**, *21* (22), 10226-10233.
- 54
55
56
57
58
59
60

- 1
2
3 42. Guo, Y.; Marchuk, K.; Sampat, S.; Abraham, R.; Fang, N.; Malko, A. V.; Vela, J., Unique
4 Challenges Accompany Thick-Shell CdSe/nCdS ($n > 10$) Nanocrystal Synthesis. *The Journal of Physical*
5 *Chemistry C* **2012**, *116* (4), 2791-2800.
- 6 43. Shynkarenko, Y.; Bodnarchuk, M. I.; Bernasconi, C.; Berezovska, Y.; Verteletskyi, V.;
7 Ochsenbein, S. T.; Kovalenko, M. V., Direct Synthesis of Quaternary Alkylammonium-Capped
8 Perovskite Nanocrystals for Efficient Blue and Green Light-Emitting Diodes. *ACS Energy Letters* **2019**, *4*
9 (11), 2703-2711.
- 10 44. Anderson, N. C.; Chen, P. E.; Buckley, A. K.; De Roo, J.; Owen, J. S., Stereoelectronic Effects on
11 the Binding of Neutral Lewis Bases to CdSe Nanocrystals. *Journal of the American Chemical Society*
12 **2018**, *140* (23), 7199-7205.
- 13 45. De Nolf, K.; Cosseddu, S. M.; Jasieniak, J. J.; Drijvers, E.; Martins, J. C.; Infante, I.; Hens, Z.,
14 Binding and Packing in Two-Component Colloidal Quantum Dot Ligand Shells: Linear *versus* Branched
15 Carboxylates. *Journal of the American Chemical Society* **2017**, *139* (9), 3456-3464.
- 16 46. Karanewsky, D. S.; Badia, M. C.; Cushman, D. W.; DeForrest, J. M.; Dejneka, T.; Loots, M. J.;
17 Perri, M. G.; Petrillo, E. W., Jr.; Powell, J. R., (Phosphinyloxy)acyl Amino Acid Inhibitors of Angiotensin
18 Converting Enzyme (ACE). 1. Discovery of (S)-1-[6-amino-2-[[hydroxy(4-phenylbutyl)phosphinyl]oxy]-
19 1-oxohexyl]-L-proline a Novel Orally Active Inhibitor of ACE. *Journal of Medicinal Chemistry* **1988**, *31*
20 (1), 204-12.
- 21 47. Troupa, P.; Katsioulari, G.; Vassiliou, S., Rapid and Efficient Microwave-Assisted
22 Hydrophosphinylation of Unactivated Alkenes with H-Phosphinic Acids without Added Metal or Radical
23 Initiator. *Synlett* **2015**, *26* (19), 2714-2719.
- 24 48. Montchamp, J.-L., Phosphinate Chemistry in the 21st Century: A Viable Alternative to the Use
25 of Phosphorus Trichloride in Organophosphorus Synthesis. *Accounts of Chemical Research* **2014**, *47*
26 (1), 77-87.
- 27 49. Deprèle, S.; Montchamp, J.-L., Triethylborane-Initiated Room Temperature Radical Addition of
28 Hypophosphites to Olefins: Synthesis of Monosubstituted Phosphinic Acids and Esters. *The Journal of*
29 *Organic Chemistry* **2001**, *66* (20), 6745-6755.
- 30 50. Sytniczuk, A.; Dąbrowski, M.; Banach, Ł.; Urban, M.; Czarnocka-Śniadała, S.; Milewski, M.;
31 Kajetanowicz, A.; Grela, K., At Long Last: Olefin Metathesis Macrocyclization at High Concentration.
32 *Journal of the American Chemical Society* **2018**, *140* (28), 8895-8901.
- 33 51. Appel, R., Tertiary Phosphane/Tetrachloromethane, a Versatile Reagent for Chlorination,
34 Dehydration, and P-N Linkage. *Angewandte Chemie International Edition in English* **1975**, *14* (12), 801-
35 811.
- 36 52. M. Crawforth, J.; Fawcett, J.; J. Rawlings, B., Asymmetric Synthesis of A-factor. *Journal of the*
37 *Chemical Society, Perkin Transactions 1* **1998**, (10), 1721-1726.
- 38 53. Jia, X.; Weber, S.; Schols, D.; Meier, C., Membrane Permeable, Bioreversibly Modified Prodrugs
39 of Nucleoside Diphosphate-γ-Phosphonates. *Journal of Medicinal Chemistry* **2020**, *63* (20), 11990-
40 12007.
- 41 54. Edmundson, R. S., Properties and Reactions of Phosphonic and Phosphinic Acids and their
42 Derivatives. In *PATAI'S Chemistry of Functional Groups*.
- 43 55. Christiansen, T. L.; Cooper, S. R.; Jensen, K. M. Ø., There's No Place Like Real-Space: Elucidating
44 Size-Dependent Atomic Structure of Nanomaterials Using Pair Distribution Function Analysis.
45 *Nanoscale Advances* **2020**, *2* (6), 2234-2254.
- 46 56. De Roo, J.; Yazdani, N.; Drijvers, E.; Lauria, A.; Maes, J.; Owen, J. S.; Van Driessche, I.;
47 Niederberger, M.; Wood, V.; Martins, J. C.; Infante, I.; Hens, Z., Probing Solvent-Ligand Interactions in
48 Colloidal Nanocrystals by the NMR Line Broadening. *Chemistry of Materials* **2018**, *30* (15), 5485-5492.
- 49 57. Abe, S.; Čapek, R. K.; De Geyter, B.; Hens, Z., Tuning the Postfocused Size of Colloidal
50 Nanocrystals by the Reaction Rate: From Theory to Application. *ACS Nano* **2012**, *6* (1), 42-53.
- 51 58. Karel Čapek, R.; Moreels, I.; Lambert, K.; De Muynck, D.; Zhao, Q.; Van Tomme, A.; Vanhaecke,
52 F.; Hens, Z., Optical Properties of Zincblende Cadmium Selenide Quantum Dots. *The Journal of Physical*
53 *Chemistry C* **2010**, *114* (14), 6371-6376.
- 54
55
56
57
58
59
60

- 1
2
3 59. McMurtry, B. M.; Qian, K.; Teglas, J. K.; Swarnakar, A. K.; De Roo, J.; Owen, J. S., Continuous
4 Nucleation and Size Dependent Growth Kinetics of Indium Phosphide Nanocrystals. *Chemistry of*
5 *Materials* **2020**, *32* (10), 4358-4368.
- 6 60. Whitehead, C. B.; Özkar, S.; Finke, R. G., LaMer's 1950 Model for Particle Formation of
7 Instantaneous Nucleation and Diffusion-Controlled Growth: A Historical Look at the Model's Origins,
8 Assumptions, Equations, and Underlying Sulfur Sol Formation Kinetics Data. *Chemistry of Materials*
9 **2019**, *31* (18), 7116-7132.
- 10 61. Prins, P. T.; Montanarella, F.; Dümbgen, K.; Justo, Y.; van der Bok, J. C.; Hinterding, S. O. M.;
11 Geuchies, J. J.; Maes, J.; De Nolf, K.; Deelen, S.; Meijer, H.; Zinn, T.; Petukhov, A. V.; Rabouw, F. T.; De
12 Mello Donega, C.; Vanmaekelbergh, D.; Hens, Z., Extended Nucleation and Superfocusing in Colloidal
13 Semiconductor Nanocrystal Synthesis. *Nano Letters* **2021**, *21* (6), 2487-2496.
- 14 62. Achorn, O. B.; Franke, D.; Bawendi, M. G., Seedless Continuous Injection Synthesis of Indium
15 Phosphide Quantum Dots as a Route to Large Size and Low Size Dispersity. *Chemistry of Materials*
16 **2020**, *32* (15), 6532-6539.
- 17 63. Čapek, R. K.; Lambert, K.; Dorfs, D.; Smet, P. F.; Poelman, D.; Eychmüller, A.; Hens, Z., Synthesis
18 of Extremely Small CdSe and Bright Blue Luminescent CdSe/ZnS Nanoparticles by a Prefocused Hot-
19 Injection Approach. *Chemistry of Materials* **2009**, *21* (8), 1743-1749.
- 20 64. Pun, A. B.; Mule, A. S.; Held, J. T.; Norris, D. J., Core/Shell Magic-Sized CdSe Nanocrystals. *Nano*
21 *Letters* **2021**, *21* (18), 7651-7658.
- 22 65. Huang, L.; Ye, Z.; Yang, L.; Li, J.; Qin, H.; Peng, X., Synthesis of Colloidal Quantum Dots with an
23 Ultranarrow Photoluminescence Peak. *Chemistry of Materials* **2021**, *33* (5), 1799-1810.
- 24 66. Anderson, N. C.; Hendricks, M. P.; Choi, J. J.; Owen, J. S., Ligand Exchange and the Stoichiometry
25 of Metal Chalcogenide Nanocrystals: Spectroscopic Observation of Facile Metal-Carboxylate
26 Displacement and Binding. *Journal of the American Chemical Society* **2013**, *135* (49), 18536-18548.
- 27 67. Hassinen, A.; Moreels, I.; De Nolf, K.; Smet, P. F.; Martins, J. C.; Hens, Z., Short-Chain Alcohols
28 Strip X-Type Ligands and Quench the Luminescence of PbSe and CdSe Quantum Dots, Acetonitrile Does
29 Not. *Journal of the American Chemical Society* **2012**, *134* (51), 20705-20712.
- 30 68. Nan, W.; Niu, Y.; Qin, H.; Cui, F.; Yang, Y.; Lai, R.; Lin, W.; Peng, X., Crystal Structure Control of
31 Zinc-Blende CdSe/CdS Core/Shell Nanocrystals: Synthesis and Structure-Dependent Optical Properties.
32 *Journal of the American Chemical Society* **2012**, *134* (48), 19685-19693.
- 33 69. Chen, O.; Zhao, J.; Chauhan, V. P.; Cui, J.; Wong, C.; Harris, D. K.; Wei, H.; Han, H.-S.; Fukumura,
34 D.; Jain, R. K.; Bawendi, M. G., Compact High-Quality CdSe–CdS Core–Shell Nanocrystals with Narrow
35 Emission Linewidths and Suppressed Blinking. *Nature Materials* **2013**, *12* (5), 445-451.
- 36 70. Jasieniak, J.; Mulvaney, P., From Cd-Rich to Se-Rich – the Manipulation of CdSe Nanocrystal
37 Surface Stoichiometry. *Journal of the American Chemical Society* **2007**, *129* (10), 2841-2848.
- 38 71. Grabolle, M.; Ziegler, J.; Merkulov, A.; Nann, T.; Resch-Genger, U., Stability and Fluorescence
39 Quantum Yield of CdSe–ZnS Quantum Dots—Influence of the Thickness of the ZnS Shell. *Annals of the*
40 *New York Academy of Sciences* **2008**, *1130* (1), 235-241.
- 41 72. Hines, M. A.; Guyot-Sionnest, P., Synthesis and Characterization of Strongly Luminescing ZnS-
42 Capped CdSe Nanocrystals. *The Journal of Physical Chemistry* **1996**, *100* (2), 468-471.
- 43 73. Bae, W. K.; Padilha, L. A.; Park, Y.-S.; McDaniel, H.; Robel, I.; Pietryga, J. M.; Klimov, V. I.,
44 Controlled Alloying of the Core–Shell Interface in CdSe/CdS Quantum Dots for Suppression of Auger
45 Recombination. *ACS Nano* **2013**, *7* (4), 3411-3419.
- 46 74. Peng, X.; Schlamp, M. C.; Kadavanich, A. V.; Alivisatos, A. P., Epitaxial Growth of Highly
47 Luminescent CdSe/CdS Core/Shell Nanocrystals with Photostability and Electronic Accessibility. *Journal*
48 *of the American Chemical Society* **1997**, *119* (30), 7019-7029.
- 49 75. Dabbousi, B. O.; Rodriguez-Viejo, J.; Mikulec, F. V.; Heine, J. R.; Mattoussi, H.; Ober, R.; Jensen,
50 K. F.; Bawendi, M. G., (CdSe)ZnS Core–Shell Quantum Dots: Synthesis and Characterization of a Size
51 Series of Highly Luminescent Nanocrystallites. *The Journal of Physical Chemistry B* **1997**, *101* (46), 9463-
52 9475.
- 53
54
55
56
57
58
59
60

- 1
2
3 76. Murray, C. B.; Norris, D. J.; Bawendi, M. G., Synthesis and Characterization of Nearly
4 Monodisperse CdE (E = Sulfur, Selenium, Tellurium) Semiconductor Nanocrystallites. *Journal of the*
5 *American Chemical Society* **1993**, *115* (19), 8706-8715.
- 6 77. Bullen, C.; Mulvaney, P., The Effects of Chemisorption on the Luminescence of CdSe Quantum
7 Dots. *Langmuir* **2006**, *22* (7), 3007-3013.
- 8 78. Campos, M. P.; Hendricks, M. P.; Beecher, A. N.; Walravens, W.; Swain, R. A.; Cleveland, G. T.;
9 Hens, Z.; Sfeir, M. Y.; Owen, J. S., A Library of Selenourea Precursors to PbSe Nanocrystals with Size
10 Distributions near the Homogeneous Limit. *Journal of the American Chemical Society* **2017**, *139* (6),
11 2296-2305.
- 12 79. Ruberu, T. P. A.; Albright, H. R.; Callis, B.; Ward, B.; Cisneros, J.; Fan, H.-J.; Vela, J., Molecular
13 Control of the Nanoscale: Effect of Phosphine–Chalcogenide Reactivity on CdS–CdSe Nanocrystal
14 Composition and Morphology. *ACS Nano* **2012**, *6* (6), 5348-5359.
- 15 80. Guo, Y.; Alvarado, S. R.; Barclay, J. D.; Vela, J., Shape-Programmed Nanofabrication:
16 Understanding the Reactivity of Dichalcogenide Precursors. *ACS Nano* **2013**, *7* (4), 3616-3626.
- 17 81. Vidal, S., Safety First: A Recent Case of a Dichloromethane Injection Injury. *ACS Central Science*
18 **2020**, *6* (2), 83-86.
- 19 82. Ménard, A. D.; Trant, J. F., A review and critique of academic lab safety research. *Nature*
20 *Chemistry* **2020**, *12* (1), 17-25.
- 21 83. Steimle, B. C.; Fagan, A. M.; Butterfield, A. G.; Lord, R. W.; McCormick, C. R.; Di Domizio, G. A.;
22 Schaak, R. E., Experimental Insights into Partial Cation Exchange Reactions for Synthesizing
23 Heterostructured Metal Sulfide Nanocrystals. *Chemistry of Materials* **2020**, *32* (13), 5461-5482.
- 24 84. Williams, D. B. G.; Lawton, M., Drying of Organic Solvents: Quantitative Evaluation of the
25 Efficiency of Several Desiccants. *The Journal of Organic Chemistry* **2010**, *75* (24), 8351-8354.
- 26 85. Doan-Nguyen, V. V.; Carroll, P. J.; Murray, C. B., Structure determination and modeling of
27 monoclinic trioctylphosphine oxide. *Acta crystallographica. Section C, Structural chemistry* **2015**, *71* (Pt
28 3), 239-41.
- 29 86. Dhaene, E.; Billet, J.; Bennett, E.; Van Driessche, I.; De Roo, J., The Trouble with ODE:
30 Polymerization during Nanocrystal Synthesis. *Nano Letters* **2019**, *19* (10), 7411-7417.
- 31 87. Maes, J.; Castro, N.; De Nolf, K.; Walravens, W.; Abécassis, B.; Hens, Z., Size and Concentration
32 Determination of Colloidal Nanocrystals by Small-Angle X-ray Scattering. *Chemistry of Materials* **2018**,
33 *30* (12), 3952-3962.
- 34 88. Akoka, S.; Barantin, L.; Trierweiler, M., Concentration Measurement by Proton NMR Using the
35 ERETIC Method. *Analytical Chemistry* **1999**, *71* (13), 2554-2557.
- 36 89. Silvestre, V.; Goupy, S.; Trierweiler, M.; Robins, R.; Akoka, S., Determination of Substrate and
37 Product Concentrations in Lactic Acid Bacterial Fermentations by Proton NMR Using the ERETIC
38 Method. *Analytical Chemistry* **2001**, *73* (8), 1862-1868.
- 39 90. Connell, M. A.; Bowyer, P. J.; Adam Bone, P.; Davis, A. L.; Swanson, A. G.; Nilsson, M.; Morris,
40 G. A., Improving the Accuracy of Pulsed Field Gradient NMR Diffusion Experiments: Correction for
41 Gradient Non-Uniformity. *Journal of Magnetic Resonance* **2009**, *198* (1), 121-131.
- 42 91. Prescher, C.; Prakapenka, V. B., DIOPTAS: a Program for Reduction of Two-Dimensional X-Ray
43 Diffraction Data and Data Exploration. *High Pressure Research* **2015**, *35* (3), 223-230.
- 44 92. Juhas, P.; Davis, T.; Farrow, C. L.; Billinge, S. J. L., PDFgetX3: a Rapid and Highly Automatable
45 Program for Processing Powder Diffraction Data into Total Scattering Pair Distribution Functions.
46 *Journal of Applied Crystallography* **2013**, *46* (2), 560-566.
- 47 93. Yang, X.; Juhas, P.; Farrow, C. L.; Billinge, S. J., xPDFsuite: an end-to-end software solution for
48 high throughput pair distribution function transformation, visualization and analysis. *arXiv preprint*
49 *arXiv:1402.3163* **2014**.
- 50 94. Juhas, P.; Farrow, C. L.; Yang, X.; Knox, K. R.; Billinge, S. J. L., Complex Modeling: a Strategy and
51 Software Program for Combining Multiple Information Sources to Solve Ill Posed Structure and
52 Nanostructure Inverse Problems. *Acta Crystallographica Section A* **2015**, *71* (6), 562-568.
- 53
54
55
56
57
58
59
60

1
2
3
4
5
6
7
8
9
10
11
12
13
14
15
16
17
18
19
20
21
22
23
24
25
26
27
28
29
30
31
32
33
34
35
36
37
38
39
40
41
42
43
44
45
46
47
48
49
50
51
52
53
54
55
56
57
58
59
60

TOC

